Testing for lightning as a source of radio bursts observed on the nightside of Venus

VIKAS S. SONWALKAR AND D. L. CARPENTER

STAR Laboratory, Stanford, CA 94305-4055

R. J. STRANGEWAY

Institute for Geophysics and Planetary Physics, University of California

Los Angeles, California 90024-1567

November 6, 1990

In certain previous studies of radio burst events recorded by the Poineer Venus Orbiting Electric Field Detector (OEFD), data were sorted for statistical purposes according to occurrence at filter band frequencies smaller than or greater than typical values ($\sim$ 100 - 1000 Hz) of the ambient electron gyrofrequency. The expectation in making this distinction was that the lowest frequency signals, at 100 Hz, were candidates for propagation through the ionosphere to the spacecraft in the whistler mode, and that the higher frequency signals (730 Hz, 5.4 kHz, 30 kHz), if of subionospheric origin, would require some different ionospheric penetration mechanism. In the present work, and on the basis of certain assumptions about the homogeneity and horizontal stratification of the Venusian nightside ionosphere, we have developed methods for case-by-case testing of the hypothesis that any particular burst event originated in subionospheric lightning. The tests, which are capable of refinement, allow prediction of the resonance cone angle, refractive index, wave dispersion, and wave polarization. The tests have been applied to data from 11 periods along 7 orbits, and are believed to represent an improved way of categorizing OEFD burst data for purposes of investigating source/propagation mechanisms. The results indicate that there are at least two main categories of burst events, one that is apparently consistent with whistler-mode propagation to the satellite, and one that is not. Assessment of the distribution of these categories in the full OEFD data base must await further analysis. More extensive testing within the categories is needed, particularly of dispersion properties and of wave polarization. Four of the five burst events that we found not consistent with the lightning hypothesis involved receptions at multiple OEFD filter band frequencies. A search for the cause of such events should include plasma mechanisms local to the spacecraft, as suggested by *Taylor and Cloutier* [1985] as well as possible mechnisms of propagation

from subionospheric sources through a highly irregular ionosphere at frequencies both above and below the gyrofrequency, as proposed by *Singh and Russell* [1986]. Some indications of the existence of a candidate local mechanism have been found in satellite data acquired near Earth [*Sonwalkar et al.*, 1990].

1. INTRODUCTION

A spirited and now protracted debate has arisen in the literature over the extent to which certain wave bursts observed on the nightside of Venus from the Pioneer Venus Satellite (PVO) can be interpreted as evidence of lightning in the Venusian atmosphere [*Russell et al.*, 1988a, b; *Russell et al.*, 1989; *Russell*, 1989; *Scarf et al.*, 1987; *Scarf and Russell*, 1988; *Taylor and Cloutier*, 1986; *Taylor et al.*, 1988; *Taylor and Cloutier*, 1988; *Taylor et al.*, 1989; *Taylor et al.*, 1985]. A key element in the debate is the fact that the orbiting electric field detector (OEFD) on PVO was limited by telemetry considerations to the measurement of signals within four narrow (~30%) frequency bands centered at 100 Hz, 730 Hz, 5.4 kHz, and 30 kHz. That limitation precluded the type of wideband spectrum analysis that in the Earth and Jovian environments has permitted researchers to distinguish relatively easily between signals of lightning origin and others that appear to originate in plasma instabilities of various kinds. Lacking the desired wideband information, the OEFD investigators designed their instrument so that, under the plasma conditions that were expected to prevail at Venus, there could be at least a limited registration of signals that might originate in lightning [*Taylor et al.*, 1979; *Scarf et al.*, 1980]. In particular, the lowest frequency channel was set at 100 Hz, low enough to be in the range of frequencies that might be expected to propagate through the Venusian ionosphere in the so-called whistler mode.

The debate thus far has been dominated by the results of statistical studies [*Russell et al.*, 1988; *Scarf et al.*, 1987; *Taylor et al.*, 1985; *Scarf and Russell*, 1988; *Taylor and Cloutier*, 1988; *Taylor and Cloutier*, 1987; *Singh and Russell*, 1986; *Russell et al.*, 1988; *Taylor et al.*, 1989; *Russell*, 1989; *Scarf and Russell*, 1983], although attention has also been given to details of the instrument response to wave bursts [*Taylor et al.*, 1979; *Scarf et al.*, 1980; *Taylor and Cloutier*, 1988], to the direction of the background magnetic field [*Scarf et al.*, 1980; *Scarf and Russell*, 1983], and to polarization analysis of signals received along individual orbits [*Scarf and Russell*, 1988]. In doing statistics, it has been recognized that because the upper limiting frequency of the whistler mode in a dense plasma is $f \sim 28B$, where f is in Hz and B is the local magnetic field magnitude in nanoteslas, waves at the OEFD frequencies 730 Hz, 5.4 kHz, and 30 kHz would regularly be in a range above the whistler-mode cutoff and thus would not be expected to propagate freely.

The present report is the result of a guest investigator study conducted by two of us in collaboration with the current Principal Investigator for the OEFD (R.S.). Our intention in undertaking the study was not to judge or even critique the positions on the OEFD data previously taken, but rather to seek new understanding. In effect, we asked: what tests could be applied to the data that

might shed new light on the origin(s) of the reported bursts? As we will show, there are several such tests. Applied to selected cases on the basis of certain assumptions about the Venusian ionosphere, they suggest that in fact there are at least two main categories of bursts, one that is consistent with a subionospheric lightning source hypothesis and one that is not.

In retrospect, it is clear why the lightning hypothesis was the first to be considered. The OEFD signals were burstlike and frequently occurred in multiple channels. A similar detector flown near Earth would be expected to respond in a similar manner to signals from lightning. But it is also the case that near Earth, burstlike waves with origins other than lightning regularly produce relatively wideband responses on satellites [*Reinleitner et al.*, 1982; *Ondoh et al.*, 1989; *Sonwalkar et al.*, 1990]. Thus in approaching the Venusian data, consideration of the possibility of multiple source mechanisms seems to be warranted.

2. ANALYSIS APPROACH

The method of analysis is based on a formalism recently developed to analyze wave data received on a satellite [*Sonwalkar*, 1986]. In this formalism the kinetic constraints arising from the physics of the medium, i.e. properties such as cutoffs, dispersion, polarization of the modes of propagation, and the kinematic constraints arising from the measurement process, i.e. motion of the satellite, response of the detector, receiver characteristics, sampling rate of the data, are explicitly taken into account to predict certain quantities that can be tested experimentally. The method may be used in situations such as that of the OEFD data in which tests of a given hypothesis that are more direct in nature are not possible due to experimental limitations. We make use of Pioneer Venus Orbiter (PVO) data on cold plasma density N_e (OETP), background vector magnetic field $\mathbf{B}_0$ (OMAG), electric field in four narrowband (OEFD) channels (100 Hz, 730 Hz, 5.4 kHz, and 30 kHz), orbiter position and motion, orientation of the spacecraft spin vector, and orientation of the electric field antenna in the spin plane. By combining these measurements with known theoretical results on wave propagation in a magnetoplasma, it is possible to devise quantitative tests of the hypothesis that impulsive subionospheric sources of electromagnetic waves are responsible for the burst-like responses in the electric field detector of the PVO.

The analysis is based on the following three assumptions.

1. The Venusian ionosphere is *spatially* uniform over length scales larger than the wavelengths(λ) in question and temporally uniform over time scales larger than the wave periods concerned.

2. The Venusian ionosphere is, on average, locally *horizontally* stratified.

3. Subionospheric wave sources are *impulsive* (wideband), occur randomly in time, and produce signals that vary randomly in intensity.

Assumption 1 is believed to be justified because the refractive index in the Venusian ionosphere is large and the wave lengths are small ($\leq$ 1km). Furthermore, the wave periods of interest are short($\leq$ 10ms). By analogy with earth's ionosphere, at least at low altitude, the Venusian ionosphere can be expected to be horizontally stratified (assumption 2). *Brace et al.* [1980] compared measurements of plasma electron density during inbound and outbound parts of orbits, and found that the nightside ionosphere of Venus is horizontally stratified to a significant degree up to $\sim$ 1000 km altitude. Assumption 3 is appropriate if the subionospheric source is lightning resembling that on Earth [*Uman*, 1987].

Our *hypothesis* that there is an impulsive source of waves in the Venusian nightside atmosphere is illustrated in Figure 1. The impulsive signals from such a source are assumed to propagate in a free space mode to a lower ionospheric boundary near 140 km altitude [*Brace et al.*, 1980], after which some penetrating portion of the signal propagates through the ionosphere to the satellite. In the ionosphere, we assume that propagation takes place in the two modes predicted by cold electron plasma propagation theory. Using this theory, one can calculate two values of refractive index, which are functions of the wave frequency (f) and of the medium parameters plasma density (N_e) and the direction and magnitude of the magnetic field ($\mathbf{B}$). In order for this theory to apply, it is necessary that the medium be uniform locally (assumption 1). For the Venusian ionosphere, and for the frequency range of interest, the ion gyrofrequencies and plasma frequencies are so small that the medium may be considered to be an electron plasma in an ambient magnetic field.

Table 1 gives values of the two refractive indices N_1 and N_2 for propagation at the four OEFD frequencies. Two limiting conditions are considered; in one the angle θ between the wave normal and $\mathbf{B}$ is 0°, in the other, 90°. The magnitude of the B field is assumed to be 20, 30, or 40 nT and the plasma density to be 10^3el-cm^{-3}, typical values reported for nightside observations near 150 km altitude. Three principal effects are evident in Table 1; (i) only one mode, N_2, called the whistler-mode, can propagate freely (i.e. the refractive index is real), (ii) for the propagating mode the refractive index is very large, $\sim$ 1000 (*Strangeway* [1990] has pointed out that the large refractive index implies that it is difficult to generate whistler-mode waves locally within the Venusian ionosphere), and (iii) the propagation is a strong function of frequency and of the wave normal angle with respect to the ambient magnetic field. In general, a wave of frequency f and wave normal angle θ will propagate freely only if $f \cos\theta < f_H$, where f_H is the electron gyrofrequency. For the propagating mode N_2, there is therefore a limiting wave normal angle θ_{res}, tabulated at the right. This angle, depending as noted upon frequency and the value of magnetic field, is such that waves with wave normal angle $\theta > \theta_{res}$ are evanescent. For typical values of magnetic field in the Venusian ionosphere, only 100 Hz and 730 Hz have a nonzero resonance cone angle (θ_{res}), so that only these two channels can be expected to register a subionospheric signal. If the wave normal angle is larger than the resonance cone angle for each of the four frequencies, both modes are heavily attenuated (i.e. $\sim$50 dB/km), and the attenuation is roughly the same at all four OEFD

frequencies (see values of N_2 for $\theta = 90°$).

Assumption 2, in conjunction with the large refractive index of the propagation mode in the ionosphere and *Snell's* law, allows us to take the local vertical direction as the direction of the wave normal. With this assumption and the known medium parameters (N_e, $\mathbf{B}_0$), cold electron plasma propagation theory [*Stix*, 1962] allows us to predict wave propagation properties for a plane wave of arbitrary frequency. We can predict the propagation behavior of an arbitrary wave, since assumption 1 permits us to consider an arbitrary wave to be composed of individual plane waves. In particular, the resonance cone angle, refractive index, wave dispersion, and wave polarization can be predicted. The known wave normal angle and the calculated resonance cone angle then provide us with a test for possible propagation from a subionospheric source. If such propagation is found possible in a particular case, the observed waves must then exhibit the dispersion and polarization predicted by theory. Dispersion is measured in terms of differences in the time of arrival of signals in different frequency channels, and polarization is measured in terms of antenna spin modulation. Assumption 3, about the impulsive nature of the source and about the randomly varying source intensity, requires us to average spin fading over several events in order to compare the observed polarization with the predicted one.

Several tests of the hypothesis of an impulsive subionospheric source can now be applied to the OEFD data from individual orbits.

1. Test of wave normal direction. In this key test the wave normal angle, a measurable quantity (from data on the **B** direction with respect to the local vertical), is compared to the predicted resonance cone angle ($\theta = \cos^{-1}(f/f_H)$) to see if whistler mode propagation is possible ($\theta < \theta_{res}$). Figure 2 shows two examples of a wave penetrating a highly refracting ionosphere from a free space region below. In both cases the magnetic field is assumed to be oriented at some angle with respect to the local vertical, while the wave normal is directed along the vertical because of the Snell's law matching requirements at the boundary. In Figure 2*a*, the wave normal direction (**k** direction) lies within the resonance cone (i.e. $\theta < \theta_{res}$), and whistler-mode propagation is expected, while in Figure 2*b*, $\theta > \theta_{res}$, and we expect strong attenuation, such as that indicated in Table 1.

2. Test of dispersion. Dispersion is a pronounced effect for whistler mode signals. We show here that the dispersion of whistler mode waves arriving at PVO from a subionospheric source should be a measurable effect in the OEFD data. If the two lowest OEFD channels, 100 Hz and 730 Hz, meet the wave normal test for whistler-mode propagation, they may be expected to exhibit differences in arrival time that are consistent with differences in the expected group velocity v_g at the two frequencies Figure 3a shows the expected group velocity in km/s vs. frequency for two wave normal angles, 0° and 40°, and for N_e=1000 el-cm^{-3} and B=30 nT. In addition, due to the 30% bandwidth of each channel, individual incident signals (assumed to be impulsive with duration $\sim$ 1 ms) should show temporal broadening. The sampling rate for data in the high-resolution mode is 250 ms. Thus the difference in arrival times for signals in the 100 Hz and 730 Hz channels and

the broadening of signals due to the finite bandwidth of each of the channels will be measurable effects if they exceed 250 ms in duration.

Figures 3b and 3c show the expected relative amplitude of whistler-mode wave pulses observed in the 100 Hz and 730 Hz channel for 0° and 40° wave normal angles respectively. The source impulse is assumed to occur at 0 s, and the whistler-mode signals are assumed to propagate a distance D=10 km(in altitude) through a medium where N_e =1000 el/cc and B =30 nT. The time difference between the leading edges of the pulses in the 100 Hz and 730 Hz channels gives the expected time difference in the arrival of the two signals (100 Hz arriving first). Figures 3b and 3c show that the time difference effect is measurable (>250 ms) at 40° wave normal angle while the pulse broadening effect in the 730 Hz channel is detectable both at 0° and at 40° wave normal angle. Another effect of the pulse broadening is that the peak intensity should be reduced. If we assume that the subionospheric source has a uniform spectrum over the 100 to 730 Hz range, then it can be shown that the amplitude of the pulse due to frequency components arriving after delay t_g is given by

$$A(t_g) = \frac{K}{\sqrt{\partial t_g / \partial f}} \tag{1}$$

The constant K depends upon the strength of the lightning stroke. Since the dispersion in the 730 Hz channel is much larger than that in the 100 Hz channel, the expected amplitude in the 730 Hz channel is comparatively lower. Figures 3b and 3c show that the peak intensity occurs at the leading edge of the pulse. Thus we can define the pulse width as the time interval between the leading edge and the time when the amplitude is reduced to 10 percent (-20 dB) of the peak value.

From equation (1), we calculate the ratio of the peak intensities in the 100 Hz and 730 Hz channels, obtaining

$$\frac{I_{peak}(100Hz)}{I_{peak}(730Hz)} = \left[\frac{(\partial t_g/\partial f)_{peak(730)}}{(\partial t_g/\partial f)_{peak(100)}}\right] \tag{2}$$

This ratio is dependent on the medium parameters and wave normal only; it is not a function of altitude, since the broadening increases in proportion to distance similarly for both channels. Note that even if the source spectrum were not uniform over the 100 - 730 Hz frequency range, the ratio should be the same for different impulses as long as the shape of the source spectrum does not vary from event to event.

As a result of the broadening, the 730 Hz signal may at higher altitudes fall below the background level, and not be detectable.

Figures 3d, 3e, and 3f show, respectively, the travel time difference between 100 Hz and 730 Hz signals, the pulse widths at the two frequencies, and the relative amplitude of the 730 Hz channel

signal with respect to the 100 Hz channel as a function of wave normal angle for Ne=1000 el/cc, background magnetic fields of 25, 30 and 35 nT, and a propagation distance D of 10 km in altitude. It is clear from Figure 3d that if we assume an ionospheric boundary at 140 km, the travel time difference effect should be detectable (> 250 ms) at 150 km or above if $\theta >\sim 15°, \sim 35°, \sim 45°$ for background magnetic field strengths of 25, 30 and 35 nT, respectively. Figure 3e shows that pulse broadening should be observable at 150 km or above for the 730 Hz channel at all wave normal angles (for B= 25 and 30 nT), while it should be observable for the 100 Hz channel only when the wave normal angle is close to the resonance cone angle. Since group delay and pulse broadening are both incremental with altitude, we do not need to know the altitude of the bottom of the ionosphere to apply these tests. Figure 3f shows that the relative intensity of 730 Hz channel signals decreases with increasing wave normal angle and decreasing magnetic field strengths. Thus at large wave normal angles, 730 Hz channel signals may drop below the background noise level and not be detectable. These figures demonstrate that dispersion effects are sensitive to both the magnetic field value and the wave normal direction. They were found to be only weakly dependent on the plasma density N_e, however.

3. Test of polarization. For each propagating cold plasma mode, and given information on **B** and electron density N_e, the polarization properties of the mode are uniquely predictable as functions of frequency and wave normal direction. In general, the polarization is elliptical. If a plane wave propagating in a given direction is intercepted by a spinning spacecraft, the recorded wave amplitude should exhibit a perfect sinusoidal variation. The phase and modulation depth of this variation can be predicted, given information on the wave normal direction and on the orientation and direction of motion of the satellite. For a plane wave, the envelope of the observed voltage [*Sonwalkar*, 1986; *Sonwalkar and Inan*, 1986]is given by

$$< V(t)V^*(t) >= \frac{1}{4}L_{eff}^2 A(1 + M\cos(2\omega_s t - \alpha)), \tag{3}$$

where M and α give the depth and phase of fading that occurs at twice the spin frequency ω_s, and are dependent only on the medium parameters N_e and **B** and the wave parameters f and θ. The amplitude parameter A depends on the medium and wave parameters as well as on the strength of the plane wave. L_{eff} is the antenna effective length. Figure 4 shows a hypothetical example of three cycles of the variation that might be expected in the case of a plane wave signal.

In the case of signals hypothesized to come from a series of impulsive subionospheric sources, each received signal is too short in duration and unpredictable in intensity to provide evidence of the fading pattern. Further, the AGC receiver aboard PVO has a decay constant(τ) of 500 ms. Thus, depending on the occurrence time of source impulses and the times at which the data are sampled, the receiver will introduce a factor $D = D_0 e^{(-t/\tau)}$. Therefore, equation (2) is modified as follows:

$$< V(t)V^*(t) >= \frac{1}{4}L_{eff}^2 D(t)A(t)(1 + M\cos(2\omega_s t - \alpha)). \quad (4)$$

where $A(t)$, and $D(t)$ are randomly varying parameters due to random variations in the intensity and occurrence patterns of the source impulses (Assumption 3).

If wave bursts occur in close succession, the randomness in their individual amplitudes and occurrence times can be averaged out, provided that the medium parameters remain constant over the averaging period. That is, if the wave normal is constant (**B** constant) and N_e is constant (or effectively, if predicted spin parameters M and α are constant) during several spin cycles, averaging the data from these cycles should permit recovery of the predicted spin pattern, i.e.

$$\{< V(t)V^*(t) >\}_{(n-cycles)} = \frac{1}{4}L_{eff}^2 \{D(t)A(t)\}_{(n-cycles)}(1 + M\cos(2\omega_s t - \alpha)). \quad (5)$$

The quantity $\{D(t)A(t)\}_{(n-cycles)}$ is assumed to average out to some constant value due to the random occurrence pattern and intensities of the assumed subionospheric sources.

A proper test of the steadiness of the wave normal is the extent to which an average of several cycles of the predicted fading replicates the expected fading for a single cycle. Of course, necessary to any successful polarization test is the occurrence of signals sufficient in number to make the averaging over several cycles meaningful. In the next section we describe application of this test to the one candidate case among 7 in which suitable conditions for averaging were present.

3. RESULTS OF DATA ANALYSIS

Our study of the PVO data included a general survey of the data from orbits 475-526 in season 3 and a detailed study of the nightside data from 7 orbits, numbers 68, 86, 501, 502, 503, 515, and 526. Five of the seven, numbers 68, 86, 502, 515, and 526 were chosen from among those that had previously been presented and discussed in the literature [*Russell et al.*, 1988; *Scarf et al.*, 1980; *Taylor et al.*, 1985; *Scarf and Russell*, 1988; *Taylor and Cloutier*, 1986; *Taylor et al.*, 1987; *Taylor and Cloutier*, 1987; *Singh and Russell*, 1986]. Case 501 was selected because it was provided by the OEFD Principal Investigator (R.S.) as an example of multifrequency burst reception, and 503 was chosen simply because it followed two others on our list.

In a typical case, the satellite spent ~16-20 minutes under nightside conditions of eclipse by the planet, moving from altitudes near 2000 km to periapsis below 170 km and back on a north-south trajectory. Bursts tended to occur in groups lasting from ~30s to ~4 minutes. On three of the orbits only one group was detected, while on four orbits there were two main groups, well separated in time. Thus a total of eleven burst groups from the seven orbits were studied. Five of the burst groups occurred below 200 km, near periapsis, while two occurred near 200 km and four above 300 km altitude. We now present the results of applying the three tests described above to the data.

The wave normal test

The upper panels of Figures 5 (a)-(k) show the electron density in el-cm$^{-3}/10^4$, the ambient magnetic field magnitude in nT/10^3, and the wave electric field in Vm^{-1}Hz$^{-1/2}$ in the OEFD channels during intervals when burstlike signals were observed. The electron density data are 12-s averages; the others represent sampling every 250 ms.

The periods displayed vary in length according to the duration of the individual groups or clusters of bursts. At the upper right above the panels are indicated the starting and ending altitudes for the interval displayed. When periapsis occurred during the interval, its time is indicated by an arrow along the upper time scale and its altitude is indicated next to the arrow.

In the lower panels of Figures 5 (a)-(k) the wave normal direction is compared with the resonance cone angle θ_{res}. The great variability of θ is due to its dependence on the direction of **B**; θ_{res} depends only upon the ratio of wave frequency to the magnitude of **B**. Whistler-mode propagation should have been possible for a given wave normal direction θ if $0° < \theta < \theta_{res}$ or if $(180° - \theta_{res}) < \theta < 180$. The resonance cone angle θ_{res} and the complementary angle $(180° - \theta_{res})$ are shown for 100 Hz and 730 Hz. In some cases, such as Figure 5 (c), the resonance cone angle was 0° for 730 Hz, and therefore is not visible on the figure. $\theta_{res} = 0°$ essentially implies that no propagation could take place at the frequency in question.

In terms of this key test, we find that the data can be divided into two broad categories, which can be further divided into two sub-categories:

(a) Data *consistent* with whistler-mode propagation from subionospheric sources.

(i) The wave normal was inside the resonance cone for the 100 Hz channel, but outside for the 730 Hz channel ($\theta_{res}(730) < \theta < \theta_{res}(100)$). Only 100 Hz was observed, as expected. The wave normal condition for the subionospheric source hypothesis was fulfilled. Four such cases were found (Figures 5 (a), (b), (d), and (j)). These occurred, respectively, on orbits 68 near 200 km altitude inbound and 200 km outbound, on orbit 86 above 400 km, and on orbit 515 above 300 km.

(ii) The wave normal was inside the resonance cone for both 100 Hz and 730 Hz, i.e. $\theta < \theta_{res}(730) < \theta_{res}(100)$. Signals were observed in the 100 Hz channel only. The wave normal condition for the subionospheric source was fulfilled. However, the hypothesized broadband nature of the source suggests that a signal should have been observed in the 730 Hz channel as well (see discussion of the dispersion test below). Two such cases were found (Figures 5 (g) and (k)). These occurred, respectively, on orbit 502 above $\sim$ 400 km and on orbit 526 below $\sim$200 km.

(b) Data *not consistent* with whistler-mode propagation from subionospheric sources.

(i) The wave normal was outside the resonance cone angle for 100 Hz (and therefore for the frequencies of the other channels), i.e. $\theta > \theta_{res}(100)$. Signals were detected in the 100 Hz channel only. Theoretically, propagation in the whistler mode was not possible. One such case was found (Figure 5(f), from orbit 501 above 350 km).

(ii) The wave normal angle was outside the resonance cone for 100 Hz ($\theta > \theta_{res}(100)$). Signals were observed at 100 Hz as well as in higher frequency channels. The observations were not consistent with whistler mode propagation. Four such cases were found (Figures 5 (c), (e), (h), (i)). These occurred, respectively, on orbits 86,501,503, and 515, at altitudes below 200 km.

One interesting point is that 100 Hz signals were observed in all the cases.

The dispersion test.

Among the cases which were consistent with the subionospheric source hypothesis according to the wave normal test (set (a) above), there were none with bursts at both 100 and 730 Hz. Pulse broadening due to dispersion might explain the absence of 730 Hz signals for the cases of Figures 5 (g) and (k) in which the wave normal condition was met for both 100 Hz and 730 Hz. On both days the magnetic field was between 30 and 40 nT. The wave normal angle was between 15° and 28° for orbit 502, and between 15° and 39° for orbit 526, giving $\frac{I_{peak}(100)}{I_{peak}(730)} \sim 100 - 1000$.

The polarization test.

The polarization test can be applied to cases in category (a) above. In several of the cases, the data were expected to show relatively deep fading. However, because of temporal fluctuations in the wave normal and corresponding changes in the expected envelope from spin cycle to spin cycle, an average over multiple predicted spin cycles preserved the single cycle pattern in only one case, that of orbit 526. In this case the wave normal condition was met (Figure 5 (k)), and now the polarization condition was also met, as illustrated in Figure 6*a* and *b*. Figure 6 (a) shows the predicted sinusoidal spin fading for a plane wave propagating with wave normal as shown in the bottom panel of Figure 5 (k), and with the plasma parameters of orbit 526. The predicted spin fading is shown by the dashed curve, while the behavior of the data is shown by the solid lines. Figure 6 (b) shows the predicted spin fading and data when both are averaged over 4 spin cycles (or over 8 fading cycles). The patterns are similar, except for a phase shift which might be explained by the slow (0.5 s) time constant of the AGC amplifier.

We note that data from this orbit were previously analyzed for polarization information by *Scarf and Russell*, [1988], using a different method, and were reported to be consistent with the whistler-mode hypothesis. In that work the amplitude of the 100 Hz signal was plotted with respect to the projection of **B** in the spacecraft spin plane.

The difficulty in other cases in doing the required averaging over spin cycles is illustrated in Figure 7. Figure 7*a* shows the predicted fading pattern and the observed data for a $\sim$ 2-minute period from orbit 86 (see also Figure 5d). Relatively deep modulation appears in both curves, but following averaging over 3 or 4 cycles, as shown in Figure 7*b*, the modulation is no longer well defined, and the satisfaction of the polarization condition cannot be determined.

The data in category (b) above were not consistent with whistler mode propagation for any of the four frequency channels. The main features of these data were:

(i) The activity was generally wideband. Four out of 5 cases listed in category (b) exhibited burstlike signals in more than one channel. The frequencies of these signals ranged from < 100 Hz to > 30000 Hz. The typical electron gyrofrequency (the nominal upper limit for whistler-mode propagation in a dense plasma) during these observations was 1000 Hz. Thus the signals were observed over a frequency range that extended from well below to well above the local gyrofrequency.

(ii) There was almost no dispersion. Orbit 501 contained many multifrequency bursts, and was suitable for study of the degree of simultaneity of the bursts in the various channels. Figure 8 shows some of the data in this case of apparently non-whistler-mode activity. The peaks in the various channels appear to be simultaneous within roughly the ~ 0.25 sec time resolution of the OEFD instrument.

(iii) A spin-averaged polarization test of the orbit 501 data showed no preferred orientation of the polarization vector.

(iv) The signals tended to occur within density troughs.

4. SUMMARY AND DISCUSSION

Beginning with the assumptions that the nightside ionosphere of Venus is uniform on a scale of $\sim$1 km and that it is locally horizontally stratified, we have used cold plasma wave propagation theory, measured medium and wave parameters, and the linear and spin motion of the satellite to develop quantitative tests of the hypothesis that plasma wave bursts observed by OEFD on the Pioneer Venus Orbiter have their origins in subionospheric lightning impulses. Given the plasma parameters of the Venusian nightside ionosphere, it was found that only one mode, the whistler-mode, could propagate at the observing frequencies of the OEFD. For individual orbits it was found possible to predict directional and frequency cutoffs, wave normal direction, group delay, pulse broadening, and polarization of waves arriving at PVO from a subionospheric source. These predicted quantities were then compared with the data from individual orbits to test the validity of the subionospheric source hypothesis. Applying this method to data from eleven periods on seven PVO nightside orbits, we found that the data fell into two categories, one consistent with the hypothesis of whistler-mode propagation from subionospheric sources (six cases) and one not consistent with that hypothesis (five cases).

Previous investigators have recognized that if the OEFD bursts are to be understood as having traversed portions of the Venusian ionosphere to the spacecraft, there must be a propagation mechanism other than the whistler mode to explain the many burst events that extend well above the electron gyrofrequency cutoff for the whistler mode [*Scarf et al.*, 1980; *Singh and Russell*, 1986]. In some statistical studies, only burst events confined to the 100 Hz channel were included, with the stated objective of focusing upon possible candidates for whistler-mode propagation [*Scarf and Russell,*, 1983, 87]. Meanwhile, in other work [*Singh and Russell*, 1986], only events with multiple

frequency character were selected, the inference being that the waves propagated to the satellite by some other mechanism. The present study has provided a way of substantially widening the physical grounds in terms of which the data are categorized, and thus offers a basis for deeper inquiry into possible source/propagation mechanisms.

Favorable possibilities for further application of the method are suggested by the distinctness with which the data thus far analyzed have been separated into categories. The wave normal test tended to provide unambiguous outcomes, and the relationship of the inferred wave normal angles to the resonance cone angle underwent few qualitative changes during the individual data intervals. Although only a small number of cases have been studied, we noted indications of what may be fundamental differences in the plasma conditions associated with the two inferred categories of data. For example, the four cases of multichannel activity that were found not consistent with whistler-mode propagation all occurred at altitudes below $\sim$ 200 km, while the six cases found consistent with that hypothesis were widely distributed in altitude. It may also be significant that in all four multichannel cases the B field direction was far from the local vertical, and that in three of these cases the field direction tended to vary rapidly. Among the seven cases in which only 100 Hz bursts occurred, six were consistent with the lightning source hypothesis and one was not. In the case of the latter, we may speculate that the 100 Hz bursts originated in the same mechanism responsible for the multichannel events, but that somehow the higher frequencies were not excited.

Until additional analysis is performed, we cannot estimate with confidence the size of the various categories identified. However, it seems reasonable at this stage to infer that while whistler-mode propagation from subionospheric lightning may explain a certain class of the OEFD burst events, other burst events may be the result of another mechanism. The latter may involve a condition of the plasma local to the orbiter, as argued by *Taylor and Cloutier* [1985] or might possibly be due to a special condition of the ionosphere that allows it to become transparent to signals from lightning that are both above and below the gyrofrequency, as proposed by *Singh and Russell* [1986]. Possibly relevant to the existence of two physically different ionospheric states, one that supports whistler mode propagation and one that does not, is the fact that on two of the orbits studied, 86 and 515 (Figures 5c, 5d, 5i, 5j), a non whistler-mode multichannel case was observed near periapsis, while events above 300 or 400 km on the same orbit agreed with the whistler-mode hypothesis.

Further assessment of the lightning source hypothesis requires additional case studies and refinement of the method of analysis. The assumption of horizontal stratification should be more accurately satisfied at lower altitudes, and any pulse broadening should be smaller (thus increasing the peak signal intensity) at lower altitudes; thus one should look at orbits when both 100 Hz and 730 Hz signals occur at altitudes $\leq$ 200 km. This choice of data would allow application of all three tests of the subionospheric source hypothesis. The availability of electron density data from OETP makes it possible to relax the assumption of horizontal stratification. A first order estimate of the tilt of the planes of stratification with respect to the local horizon can be obtained by comparing

electron densities at the same altitude on inbound and outbound parts of an orbit. This would lead to a more precise determination of the wave normal angle θ (by Snell's law, the wave normal is perpendicular to the plane of stratification as long as $N_2 >> 1$). The polarization test could be improved by noting that even though the fading parameters M and α are functions of the medium parameters and the wave normal angle, the functional form of equation (5) remains the same. Thus we can statistically average data over varying medium parameters and wave normal angles (from a single orbit as well as from different orbits), provided that the data are normalized with respect to the fading parameters M and α. This kind of data averaging would increase the number of data points available to test for the sinusoidal variation expected as a consequence of the wave polarization. It would also be appropriate to relax our assumption of ionospheric homogeneity, and to consider the possibility of propagation through an irregular medium to the spacecraft at frequencies both above and below the gyrofrequency.

There are indications that a search for a non-lightning source for certain events may be rewarding. Wideband dispersionless wave bursts have been found to be a common feature of satellite observations near Earth [*Ondoh et al.*, 1989; *Sonwalkar et al.*, 1990], and bursts of this general type have also been reported near the Earth's magnetopause [*Reinleitner et al.*, 1982, 83] and in the environments of Jupiter and Saturn [*Reinleitner et al.*, 1984]. These burst emissions have several characteristics common to multichannel bursts observed on PVO [*Sonwalkar et al.*, 1990]. They are impulsive and show very little or no dispersion, their frequency ranges from well below to well above the local gyrofrequency, and there is an indication that their wave normal direction may be perpendicular to the local geomagnetic field. If these signals were sampled by a receiver similar to the one on PVO, their temporal and spectral characteristics would be similar to those observed on PVO orbits such as 501 (Figure 5e). Near earth these signals have been observed on both electric and magnetic field antennas, and have been detected in the low density region outside the plasmapause at all local times [*Sonwalkar et al.*, 1990]. They show no association with terrestrial lightning (the spectral signature of lightning in these regions of the earth's magnetosphere is reasonably well understood). The signals were initially interpreted as electrostatic noise generated by a resistive medium instability [*Reinleitner et al.*, 1983]. This instability is triggered by a beam of few-hundred-eV electrons, which could be generated by electrons trapped by the wave fields of natural chorus or hiss emissions. However, the observation of a magnetic component for these bursts has called this mechanism into question [*Sonwalkar et al.*, 1990]. In summary, there is reason to believe that at least one additional source mechanism, unrelated to lightning, may be found for some of the OEFD bursts.

Another perspective on the apparently non-propagated class of PVO radio bursts is suggested by work on plasma transition regions. A recent study [*Eastman*, 1989] points out that such regions abound in space and astrophysical plasmas. Called plasma boundary layers, the regions are characterized by (1) high spatial gradients Δn, $\Delta \mathbf{B}_0$, ΔT and $\Delta \mathbf{V}$, (2) enhanced wave activity

with low-and-high-frequency electrostatic and electromagnetic emissions, (3) changes in plasma β, high to low or low to high, (4) multicomponent and anisotropic velocity distributions $f(\mathbf{V})$. The fact that the Venusian plasma conditions are highly variable in time and by inference, in space, as detected by PVO, suggests that some of the wideband bursts near Venus may be boundary layer phenomena and may thus originate in mechanisms similar to those that are active in other plasma transition regions.

5. References

Brace, L. H., R. F. Theis, W. R. Hoegy, J. H. Wolfe, J. D. Mihalov, C. T. Russell, R. C. Elphic, and A. F. Nagy, The dynamic behavior of the Venus ionosphere in response to solar wind interactions, *J. Geophys. Res., 85,* 7663, 1980.

Eastman, T. E., Transition regions in solar system and astrophysical plasmas, Accepted for publication in *IEEE Trans. on Plasma Sci.*, September, 1989.

Ondoh, T., Y. Nakamura, S. Watanabe, K. Aikyo, M. Sato, and F. Sawada, Impulsive plasma waves observed by the DE 1 in the nightside outer radiation zone, *J. Geophys. Res., 94,* 3779, 1989.

Reinleitner, L. A., D. A. Gurnett, and T. E. Eastman, Electrostatic bursts generated by Electrons in Landau resonance with whistler mode chorus, *J. Geophys. Res., 88,* 3079, 1983.

Reinleitner, L. A., W. S. Kurth, and D. A. Gurnett, Chorus-related electrostatic bursts at Jupiter and Saturn, *J. Geophys. Res., 89,* 75, 1984.

Russell, C. T., M. von Dornum, and F. L. Scarf, The altitude distribution of impulsive signals in the night ionosphere of Venus, *J. Geophys. Res., 93*, 5915, 1988a.

Russell, C. T., M. von Dornum, and F. L. Scarf, Planetographic clustering of the low-altitude impulsive electric fields in the night ionosphere of Venus, *Nature, 331,* 591, 1988b.

Russell, C. T., M. von Dornum, and R. J. Strangeway, VLF bursts in the night ionosphere of Venus: Estimates of poynting flux, *Geophys. Res. Lett., 16*, 579, 1989.

Russell, C. T., reply, *J. Geophys. Res., 94*, 12093, 1989.

Scarf, F. L., W. W. L. Taylor, C. T. Russell, and L. H. Brace, Lightning on Venus: Orbiter detection of whistler signals, *J. Geophys. Res., 85*, 8158, 1980.

Scarf, F. L. and C. T. Russell, Lightning measurements from the Pioneer Venus Orbiter, *Geophys. Res. Let., 12*, 1192, 1983.

Scarf, F. L., K. F. Jordan, and C. T. Russell, Distribution of whistler mode bursts at Venus, *J. Geophys. Res., 92*, 12411, 1987.

Scarf, F. L. and C. T. Russell, Evidence of lightning and volcanic activity on Venus: Pro and Con, *Science, 240*, 222, 1988.

Singh, R. N., and C. T. Russell, Further evidence of lightning on Venus, *Geophys. Res. Lett., 13*, 1051, 1986.

Sonwalkar, V. S., New signal analysis techniques and their applications in Space Physics, Ph.D. thesis, Stanford University, 1986.

Sonwalkar, V. S., and U. S. Inan, Measurement of Siple transmitter signals on the DE 1 satellite: wave normal direction and antenna effective length, *J. Geophys. Res., 91*, 154, 1986.

Sonwalkar, V. S., R. A. Helliwell, and U. S. Inan, Wideband VLF electromagnetic bursts observed on the DE 1 satellite, *Geophys. Res. Lett., 17,* 1861, 1990.

Stix, T. H., The theory of plasma waves, *McGraw-Hill*, 1962.

Strangeway, R. J., Radioemissions disputed, *Nature, 345*, 213, 1990.

Taylor, H. A. Jr., J. M. Grebowsky, and Paul S. Cloutier, Venus nightside ionospheric troughs: Implications for evidence of lightning and volcanism, *J. Geophys. Res., 90*, 7415, 1985.

Taylor, H. A., Jr., and Paul A. Cloutier, Venus: dead or alive?, *Science, 234*, 1087, 1986.

Taylor, H. A. Jr., Paul S. Cloutier, and Zirao Zheng, Venus "lightning" signals reinterpreted as in situ plasma noise, *J. Geophys. Res., 92*, 9907, 1987.

Taylor, H. A., Jr., and Paul A. Cloutier, Comment on "Further evidence for lightning at Venus, *Geophys. Res. Let., 14*, 568, 1987.

Taylor, H. A., Jr., and Paul A. Cloutier, Telemetry interference incorrectly interpreted as evidence for lightning and present-day volcanism at Venus, *Geophys. Res. Let., 15*, 729, 1988.

Taylor, H. A., Jr., L. Kramer, and P. A. Cloutier, Comment on "Distribution of whistler mode bursts at Venus" by F. L. Scarf, K. F. Jordan, and C. T. Russell, *J. Geophys. Res., 94*, 12087, 1989.

Taylor, W. W. L., F. L. Scarf, and C. T. Russell, Evidence for lightning on Venus, *Nature, 279*, 614, 1979.

Uman, M. A., The lightning discharge, *Academic Press*, Orlando, 1987.

FIGURE CAPTIONS

Figure 1. Possible propagation paths from a subionospheric source of electromagnetic radiation to Pioneer Venus Orbiter (PVO).

Figure 2. (a) A wave incident on the ionosphere from a subionospheric source when wave normal angle θ is less than the resonance cone angle, θ_{res}. In this case the wave can propagate in the ionosphere. (b) case when $\theta < \theta_{res}$. The wave in the ionosphere is evanescent.

Figure 3. Effects of whistler mode dispersion: (a) Whistler-mode group velocity as a function of frequency for 0° (solid line) and 40° (dashed line) wave normal angles, B=30 nT, and N_e=1000 el/cc. (b), (c) the arrival times and amplitudes of pulses after propagating a distance D = 10 km for 0° and 40° wave normals, respectively. (d), (e), (f) the difference in arrival times of 100 Hz and 730 Hz signals, pulse widths and relative peak amplitudes of signals in 730 Hz channel compared to that in 100 Hz channel as a function of wave normal angle for three values of magnetic field (25, 30, 35 nT). The electron density is assumed to be 1000 el/cc and the whistler mode wave is assumed to propagate distance of 10 km. The dashed horizontal lines in Figures (d) and (f) show the temporal resolution (250 ms) limited by sampling rate.

Group delay, pulse broadening, and ratio of peak intensities at 100 and 730 Hz as a function of wave normal angle for B = 30 nT and B = 40 nT respectively. The dashed vertical lines give the resonance cone angle and

Figure 4. Schematic of the voltage received on a spinning satellite for a plane wave. The fading parameter M and α are functions of medium parameters, wave frequency, wave normal angle with respect to **B**, spin axis, and phase of the antenna vector in the spin plane.

Figure 5. (a)-(k), Top panel shows plasma waves observed in the four OEFD channels (250 ms samples), magnetic field measured by OMAG, and electron density measured by OETP instruments. The bottom panel gives the wave normal angle with respect to local magnetic field direction. The dashed curves give the resonance cone angles for 100 Hz and 730 Hz. Propagation is allowed only for wave normal angle θ such that $0 \leq \theta < \theta_{res}$ or $(180° - \theta_{res}) < \theta \leq 180°$. In some of the figures, the resonance cone angle for 730 Hz is 0° indicating no propagation is possible at any wave normal angle.

Figure 6. (a) The predicted spin fading for the 100 Hz signal at 09:28:55 UT for orbit 526 when the wave normal direction was fairly steady (Figure 4 (k)). (b) The predicted spin fading and data averaged over four spin cycles. The spin period is 12 s. Well defined spin fading at twice the spin frequency, as predicted theoretically is seen in the averaged data.

Figure 7. (a) The predicted spin fading for 100 Hz signals during orbit 086. (b) The averaged spin fading does not show well defined spin fading at twice the spin fading, indicating the conditions necessary for the application of polarization test are not met.

Figure 8. Display on an expanded time scale of a close correlation among the plasma wave data in four frequency channels for orbit 501. Based on the wave normal test (Figure 4 (e)), these signals have not propagated in the whistler mode and therefore are not consistent with hypothesis of subionospheric source. Also note that, within the temporal resolution of 250 ms set by sampling rate, they show very little or no dispersion.

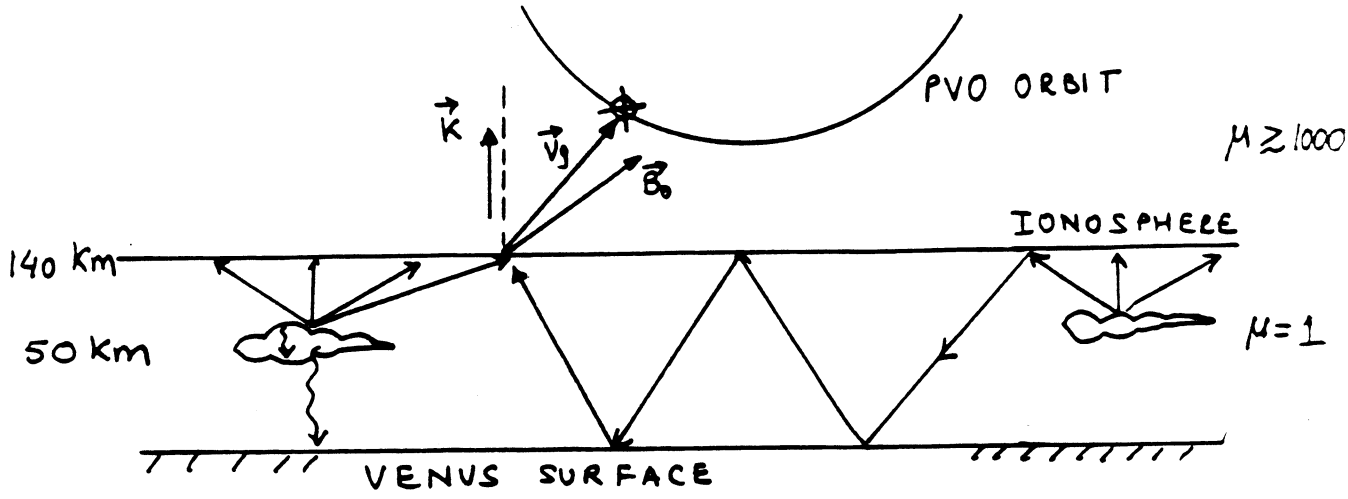

FIGURE 1 : Possible propagation path from a source of e_M. radiation below the ionosphere to PVO.

TABLE 1

B=20 nT	THETA=0		THETA=90		$N_2(\theta res)$
Freq.(Hz)	N1	N2	N1	N2	
100	1107i	1322	2840i	2864i	79°
	20.14 dB/km	λ = 2.27 km	51.68 dB/km	52.12 dB/km	
730	292i	805i	389i	389i	0°
	37.96 dB/km	104.65 dB/km	50.57 dB/km	50.57 dB/km	
5400	55i	50i	52i	52i	0°
	53.9 dB/km	49.00 dB/km	50.96 dB/km	50.96 dB/km	
30000	9.3i	9.5i	9.4i	9.4i	0°
	50.78 dB/km	51.87 dB/km	51.32 dB/km	51.32 dB/km	
B=30 nT					
100	928i	1041	2840i	2896i	83.16°
	16.88 dB/km	λ = 2.88 km	51.68 dB/km	52.70 dB/km	
730	265i	1002	389i	389i	29.65°
	34.45 dB/km	λ = 0.41 km	50.57 dB/km	50.57 dB/km	
5400	49i	57i	53i	53i	0°
	48.02 dB/km	55.86 dB/km	51.94 dB/km	51.94 dB/km	
30000	9.3i	9.5i	9.4i	9.4i	0°
	50.78 dB/km	51.87 dB/km	51.32 dB/km	51.32 dB/km	
B=40 nT					
100	815i	886	2840i	2942i	84.87°
	14.83 dB/km	λ = 3.38 km	51.68 dB/km	53.54 dB/km	
730	244i	532	389i	389i	49.32°
	31.72 dB/km	λ = 0.77 km	50.57 dB/km	50.57 dB/km	
5400	58i	59i	52i	52i	0°
	47.04 dB/km	57.82 dB/km	50.96 dB/km	50.96 dB/km	
30000	9.2i	9.6i	9.4i	9.4i	0°
	50.23 dB/km	52.42 dB/km	51.32 dB/km	51.32 dB/km	

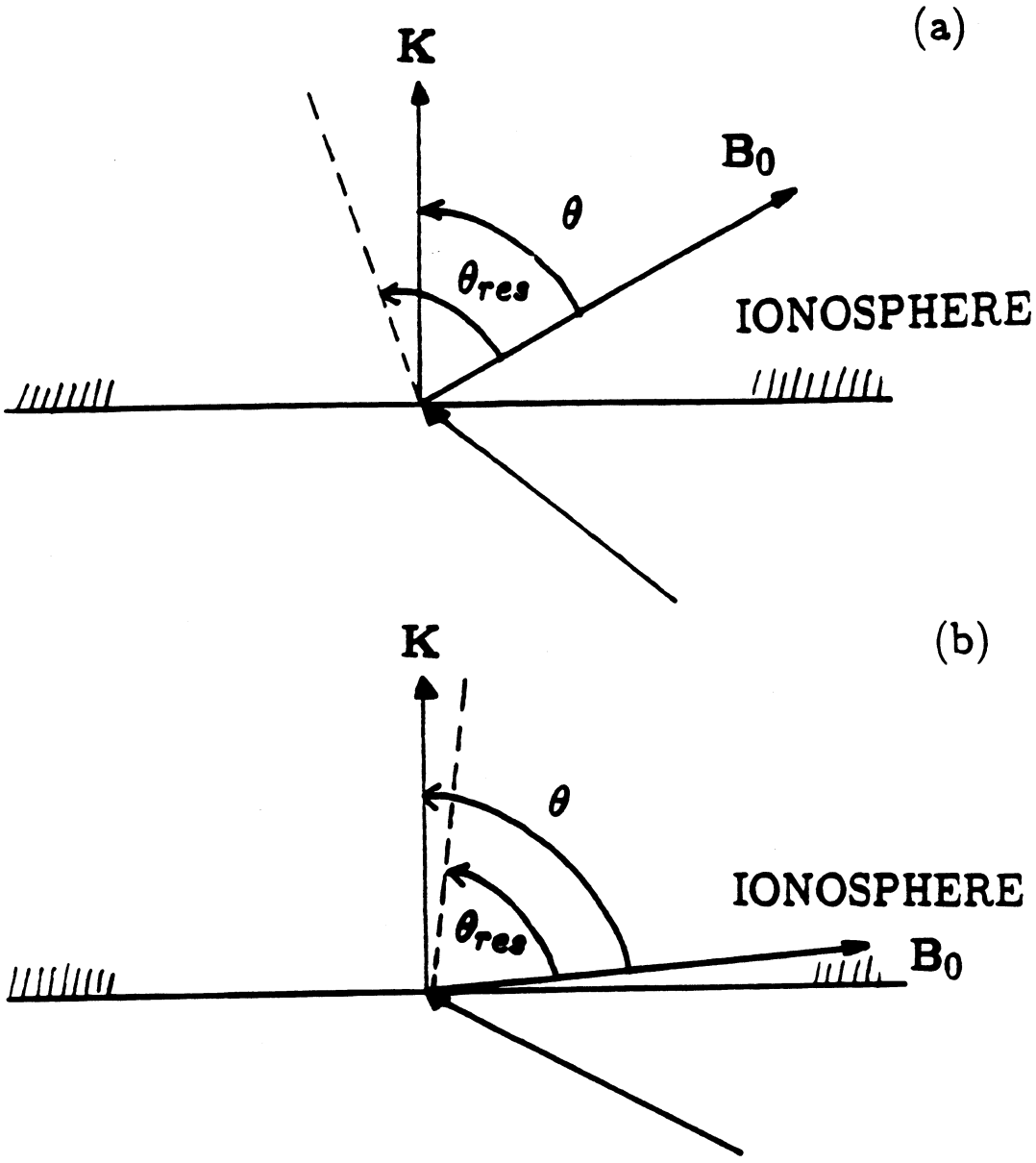

Figure 2. (a) A wave incident on the ionosphere from a source below when wave normal angle, θ is less than the resonance cone angle, θ_{res}. In this case the wave can propagate in the ionosphere. (b) case when $\theta < \theta_{res}$. The wave in the ionosphere is evanescent.

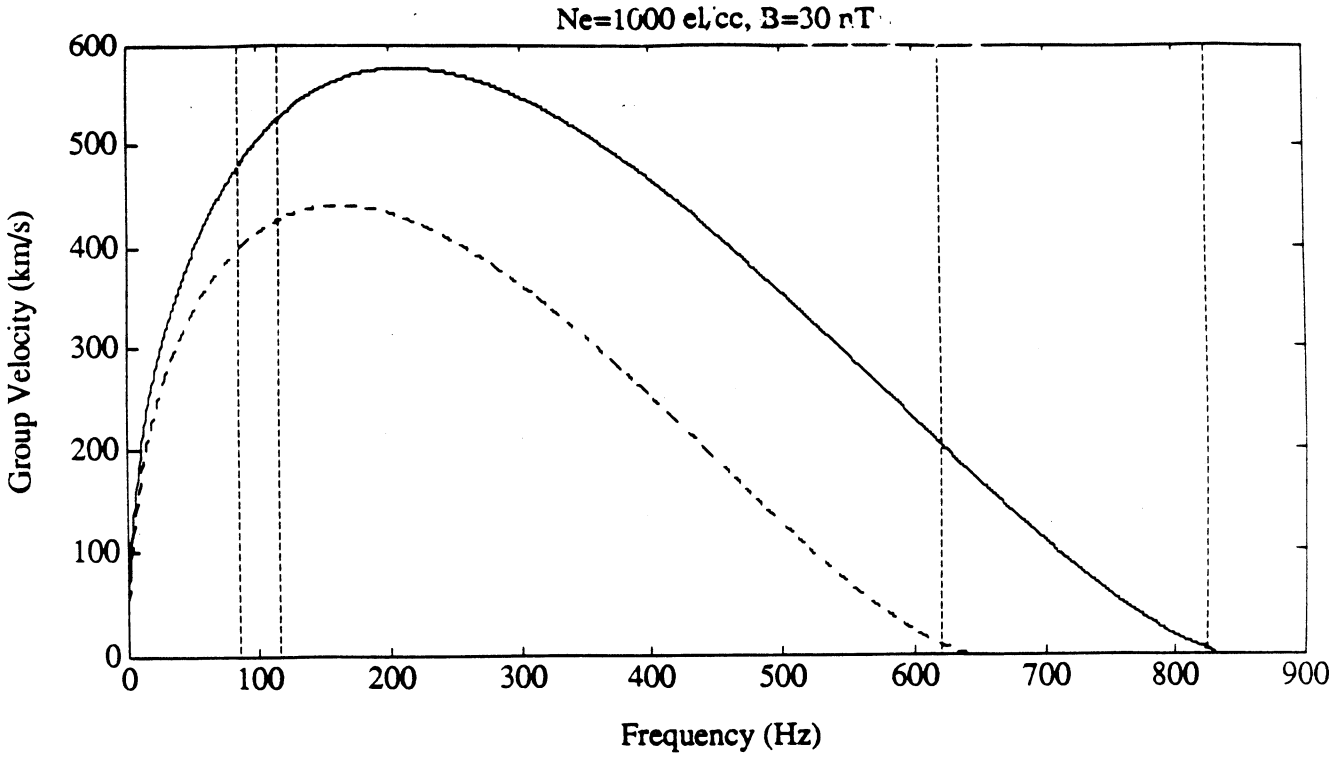
Ne=1000 el/cc, B=30 nT
Group Velocity (km/s)
Frequency (Hz)
0
100
200
300
400
500
600
700
800
900

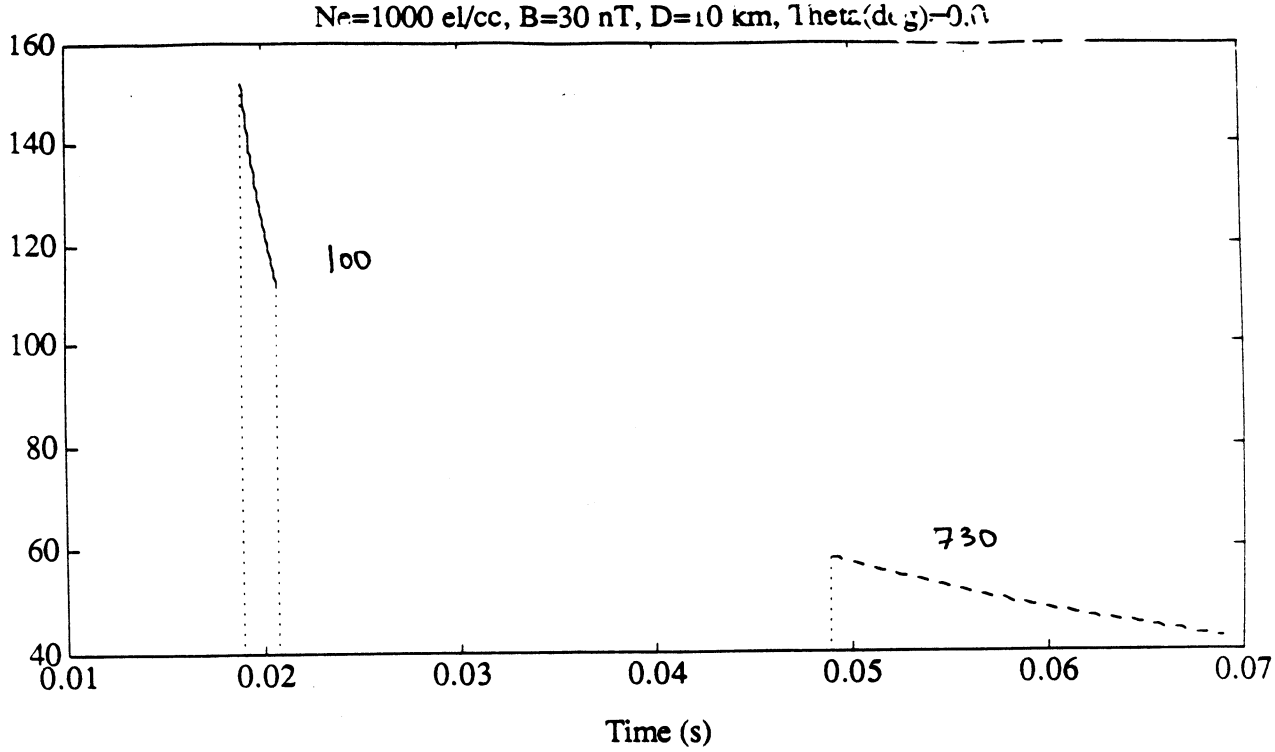
Ne=1000 el/cc, B=30 nT, D=10 km, Theta(deg)=0.0
160
140
120
100
80
60
40
0.01
0.02
0.03
0.04
0.05
0.06
0.07
Time (s)
100
730

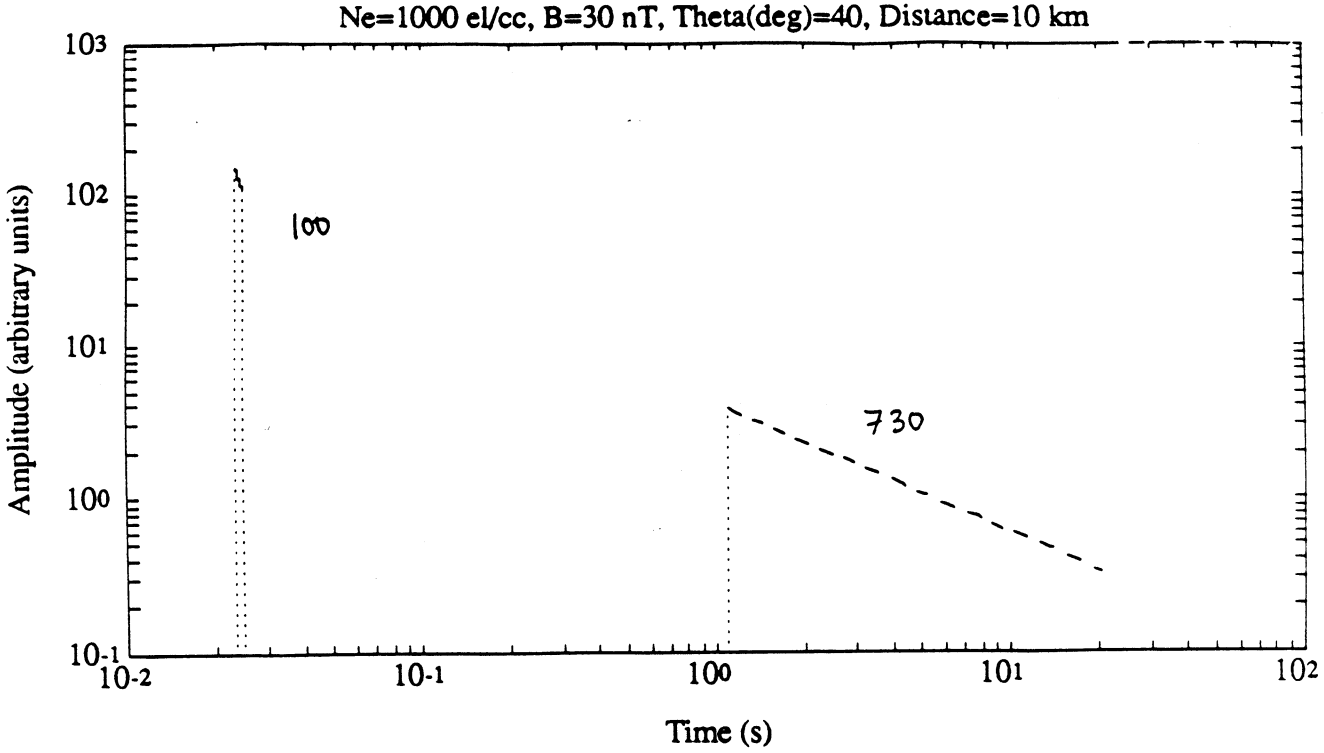
Ne=1000 el/cc, B=30 nT, Theta(deg)=40, Distance=10 km
Amplitude (arbitrary units)
10³
10²
10¹
10⁰
10⁻¹
10⁻²
10⁻¹
10⁰
10¹
10²
Time (s)
100
730

3d

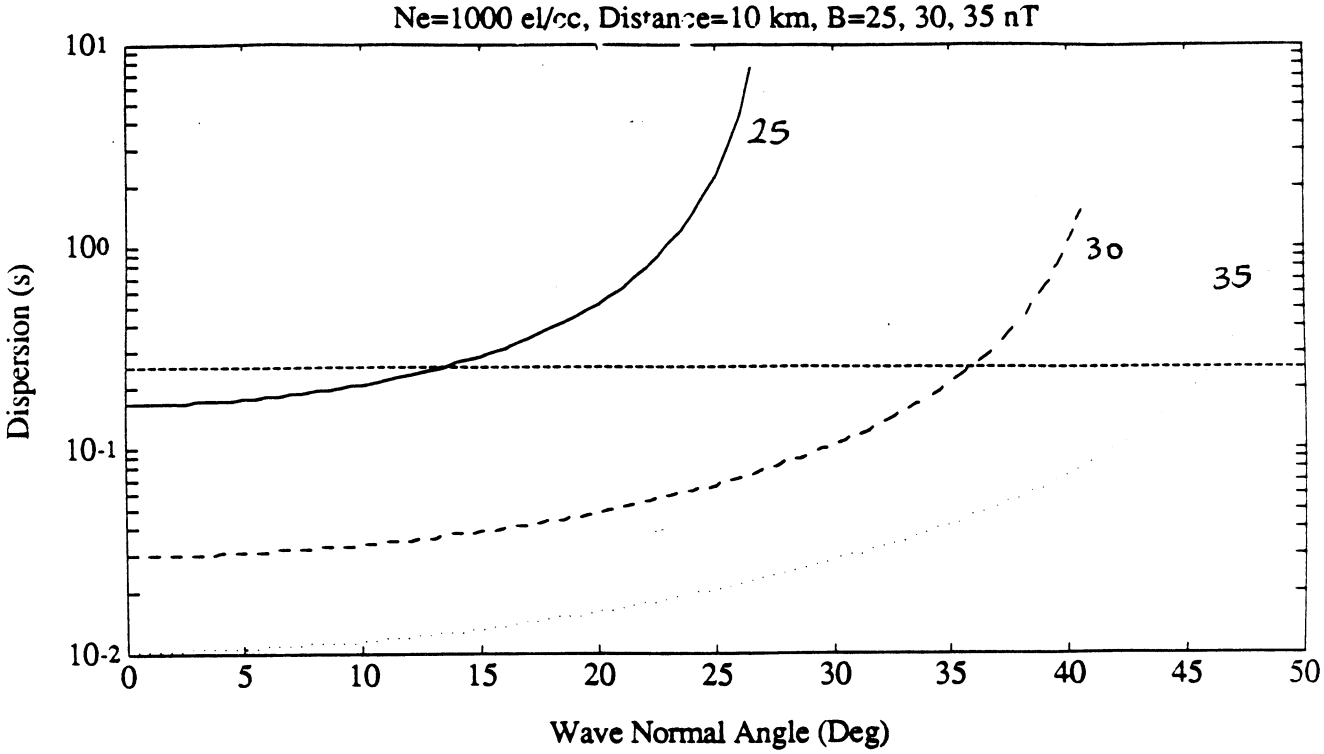
Ne=1000 el/cc, Distance=10 km, B=25, 30, 35 nT
Dispersion (s)
10¹
10⁰
10-1
10-2
0
5
10
15
20
25
30
35
40
45
50
Wave Normal Angle (Deg)
25
30
35

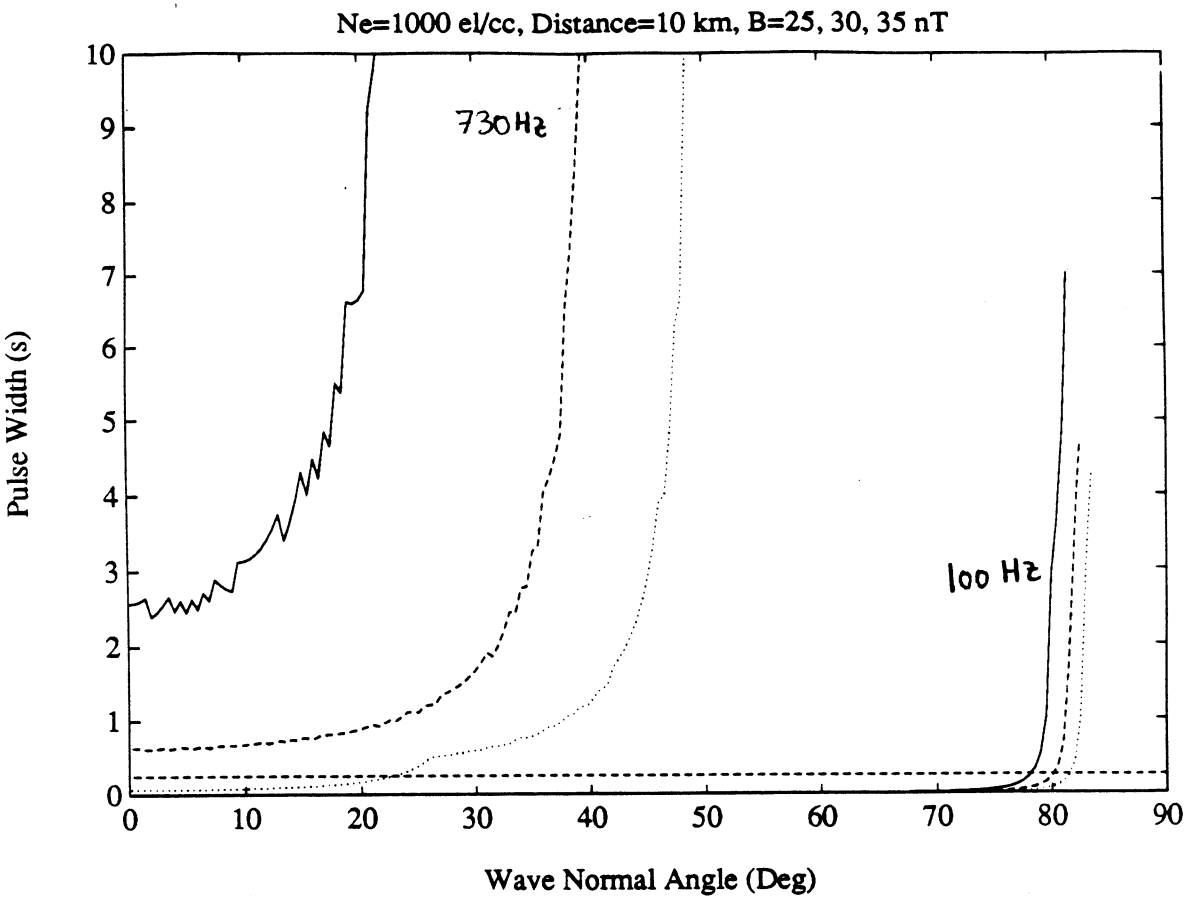
Ne=1000 el/cc, Distance=10 km, B=25, 30, 35 nT
730 Hz
100 Hz
Pulse Width (s)
Wave Normal Angle (Deg)
0
1
2
3
4
5
6
7
8
9
10
0
10
20
30
40
50
60
70
80
90

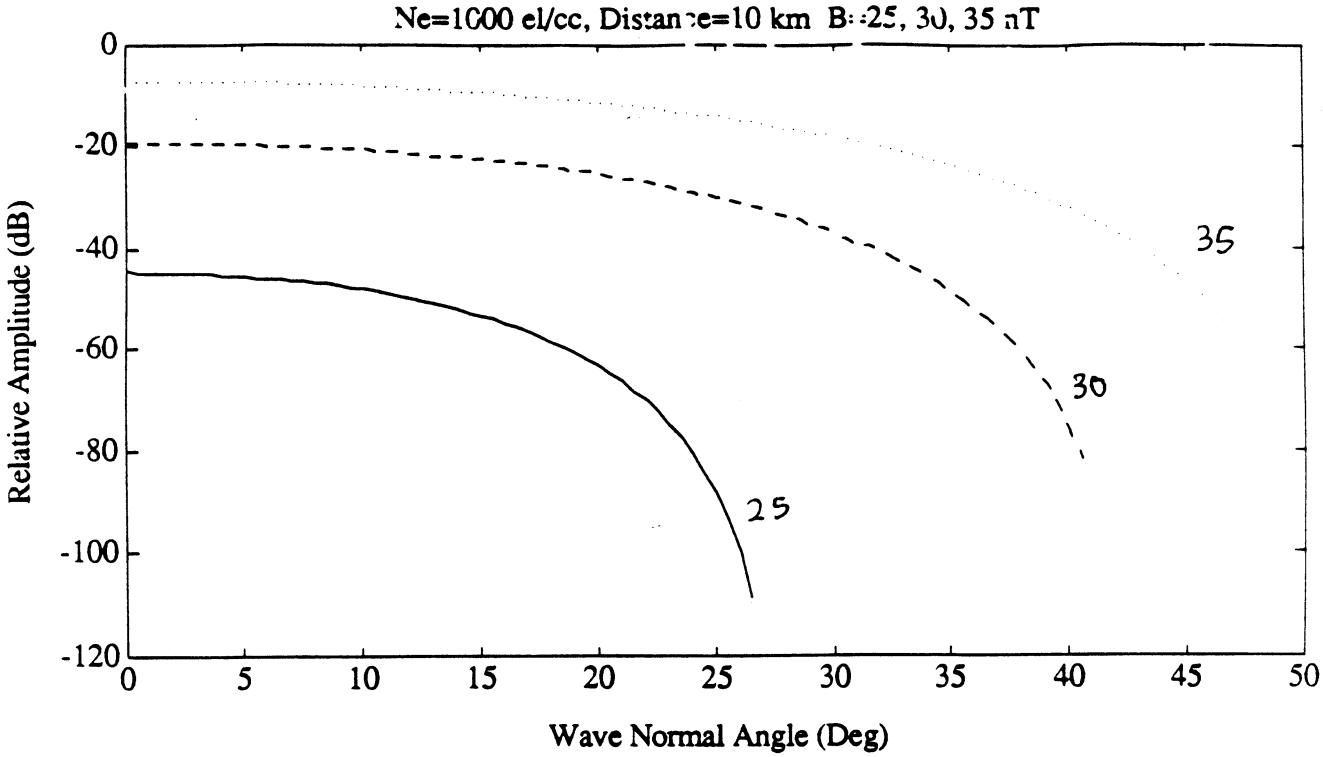
Ne=1000 el/cc, Distance=10 km B=25, 30, 35 nT
Relative Amplitude (dB)
0
-20
-40
-60
-80
-100
-120
0
5
10
15
20
25
30
35
40
45
50
Wave Normal Angle (Deg)
35
30
25

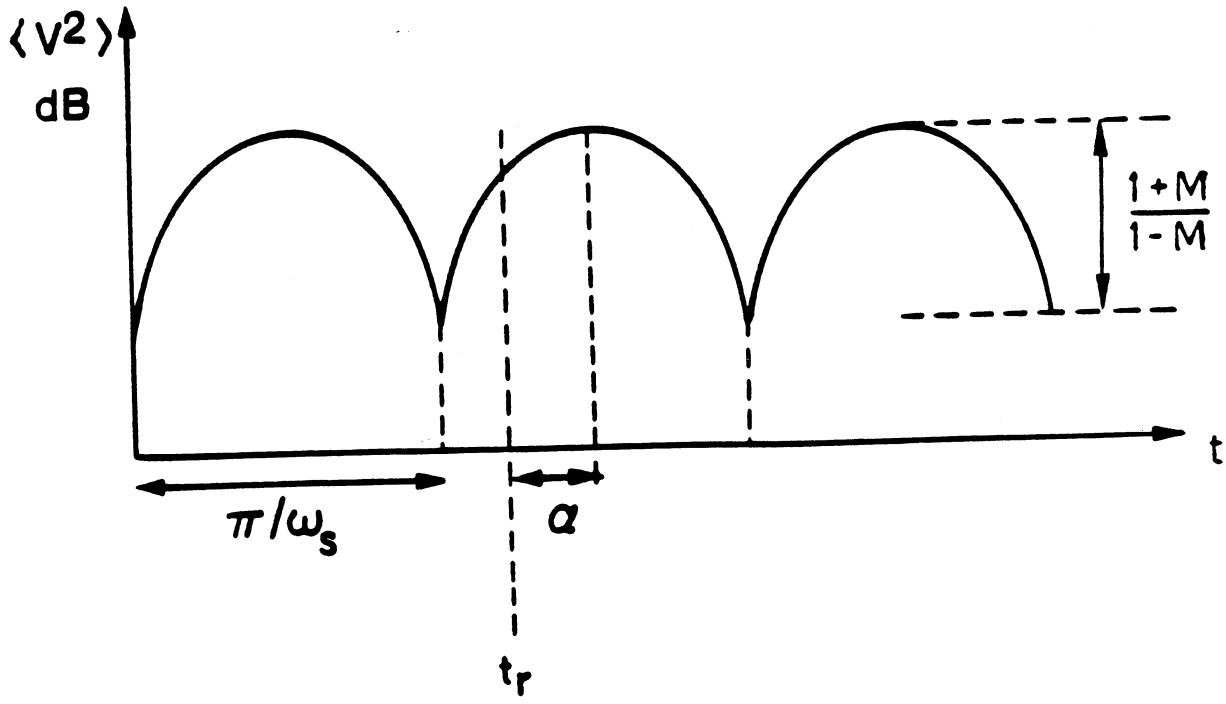

Figure 4. Schematic of the Voltage Received on a Spinning Satellite for a Plane Wave.

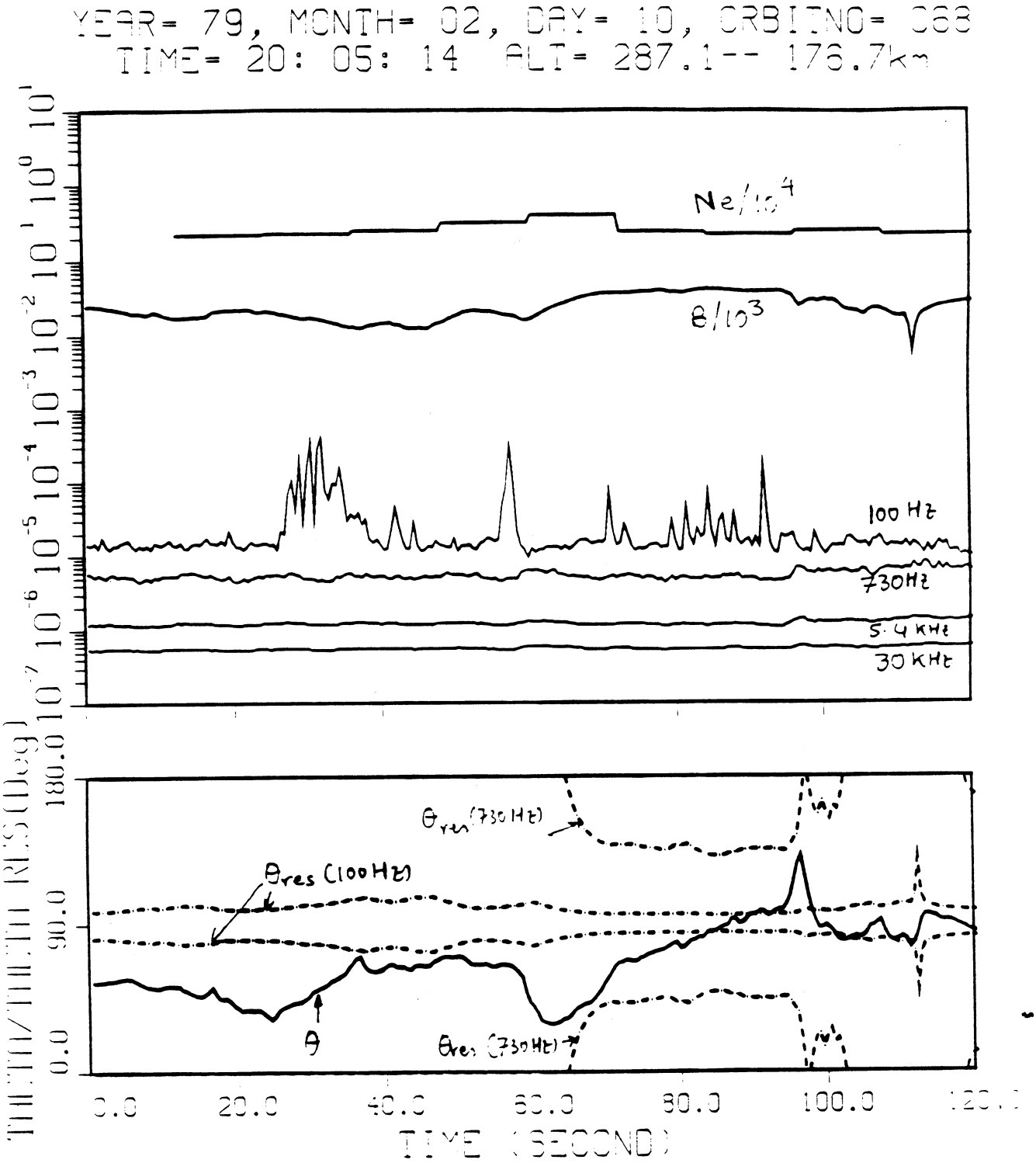

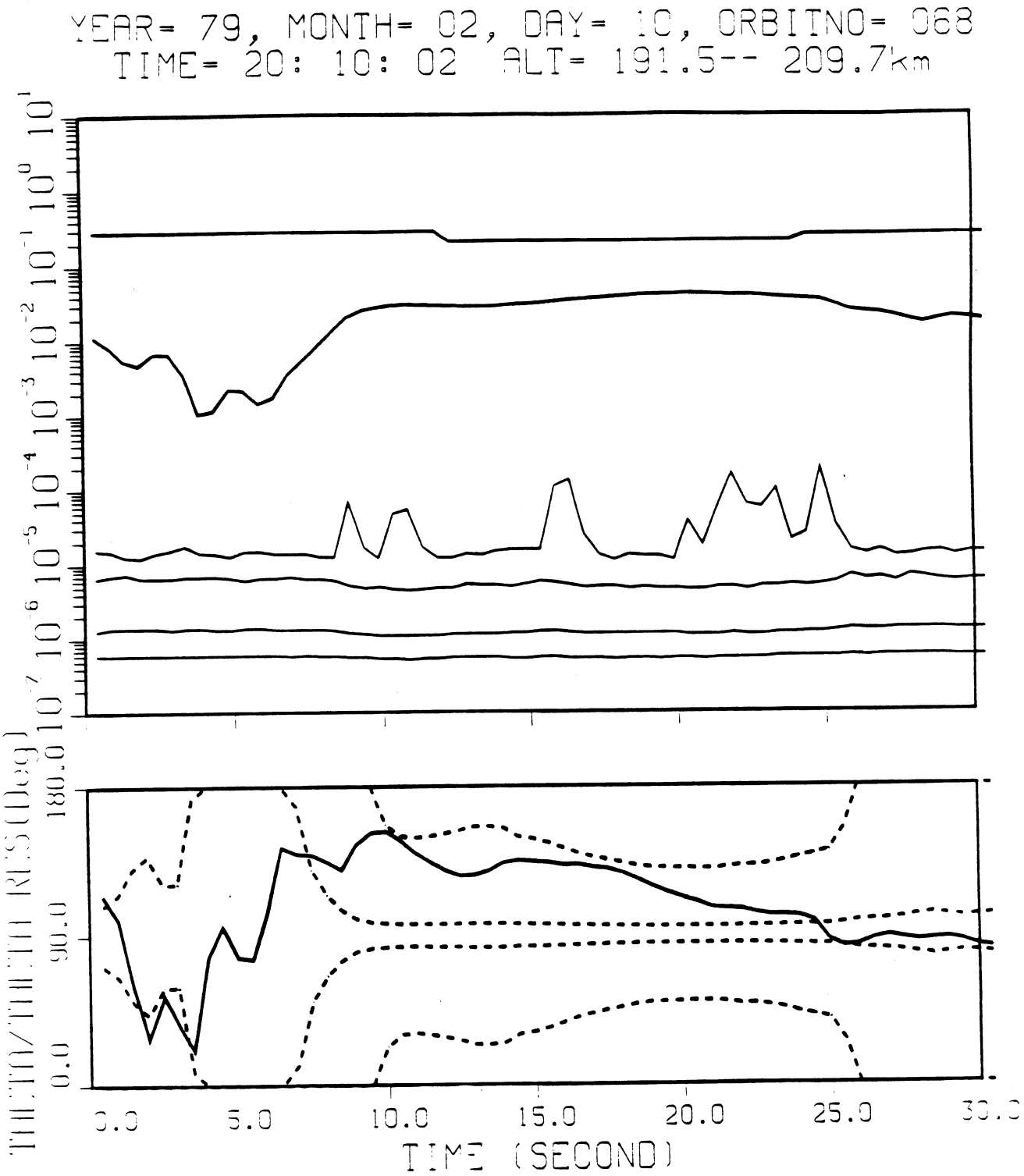

Fig 5c

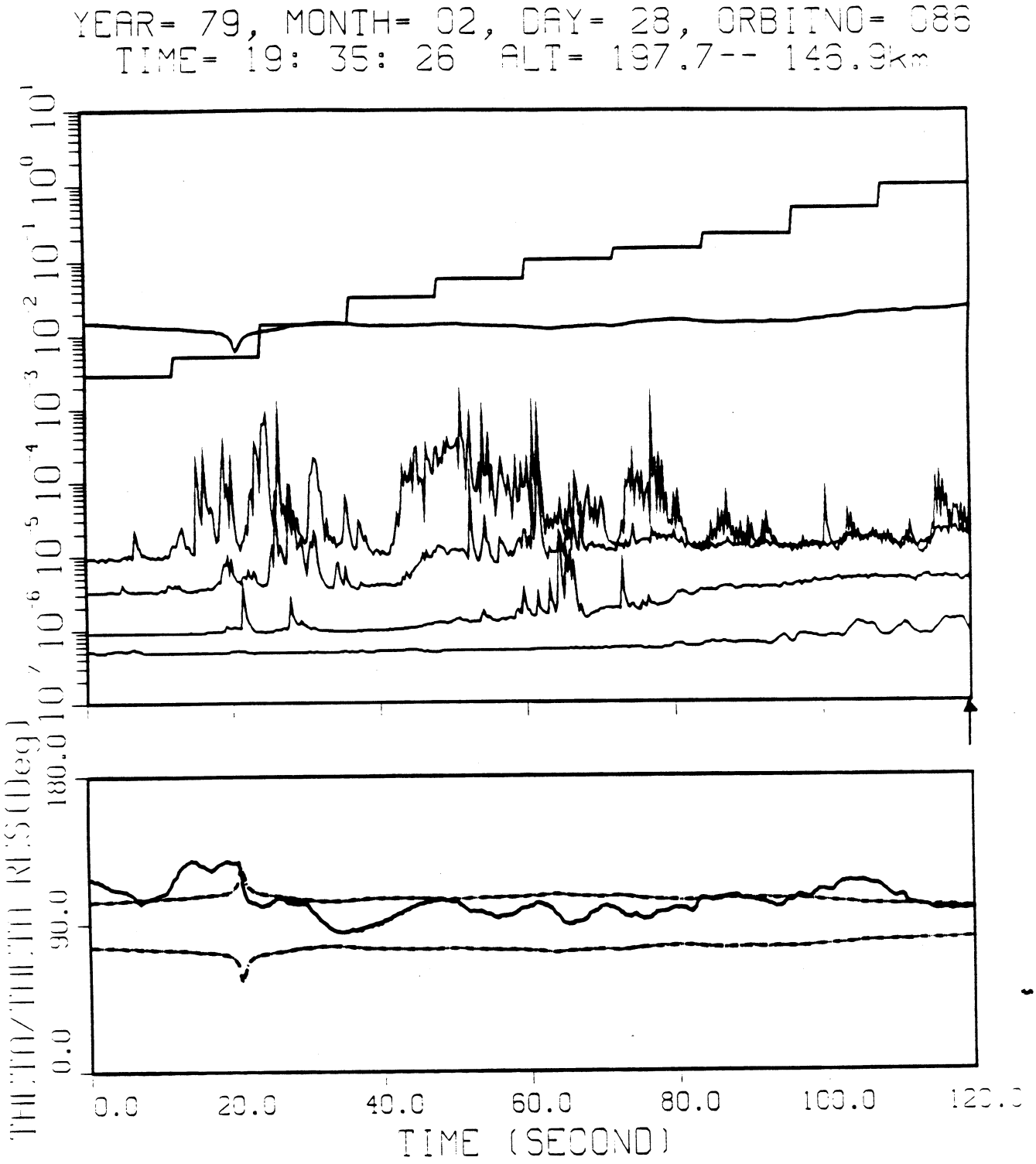

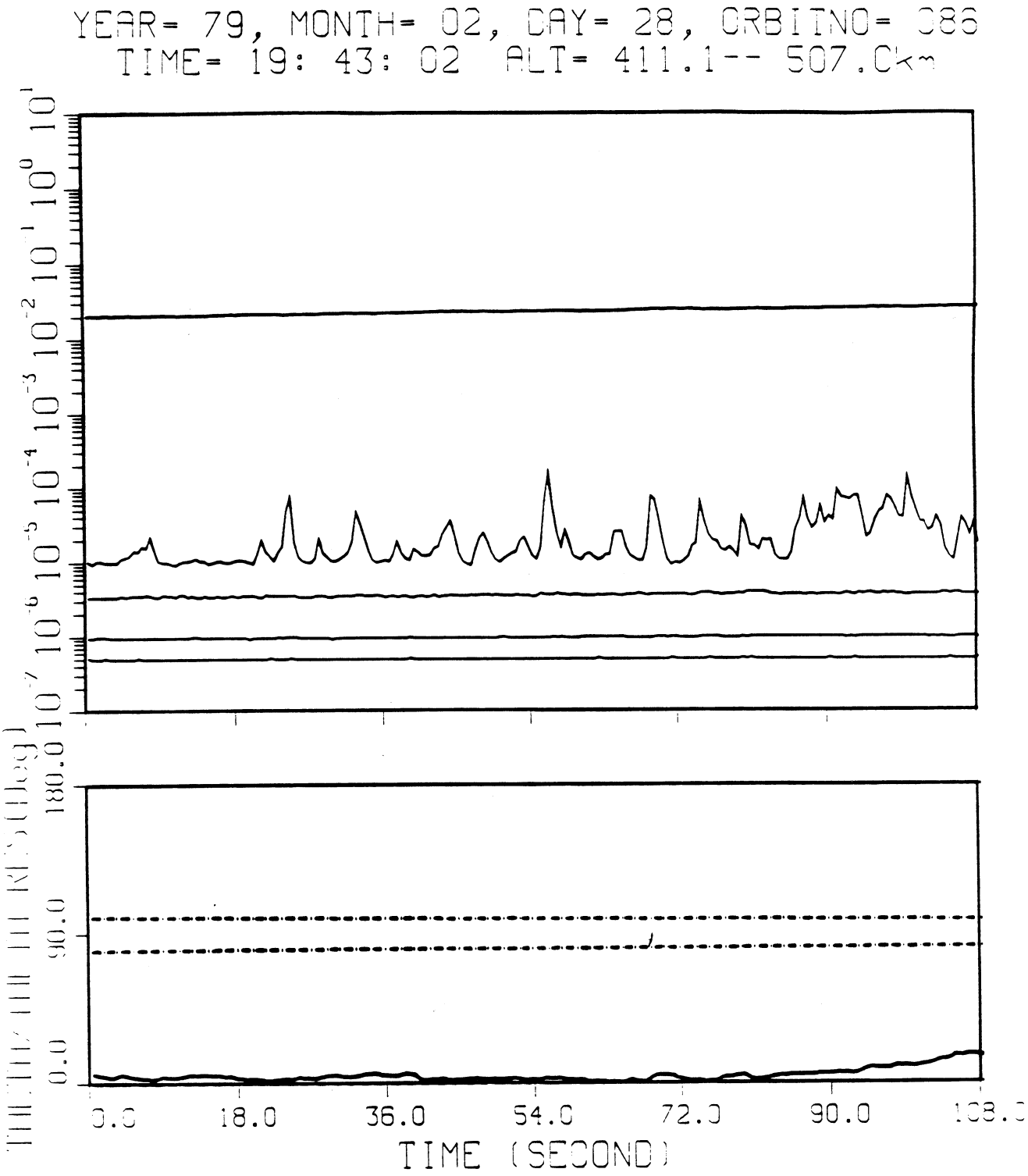

Fig 9e

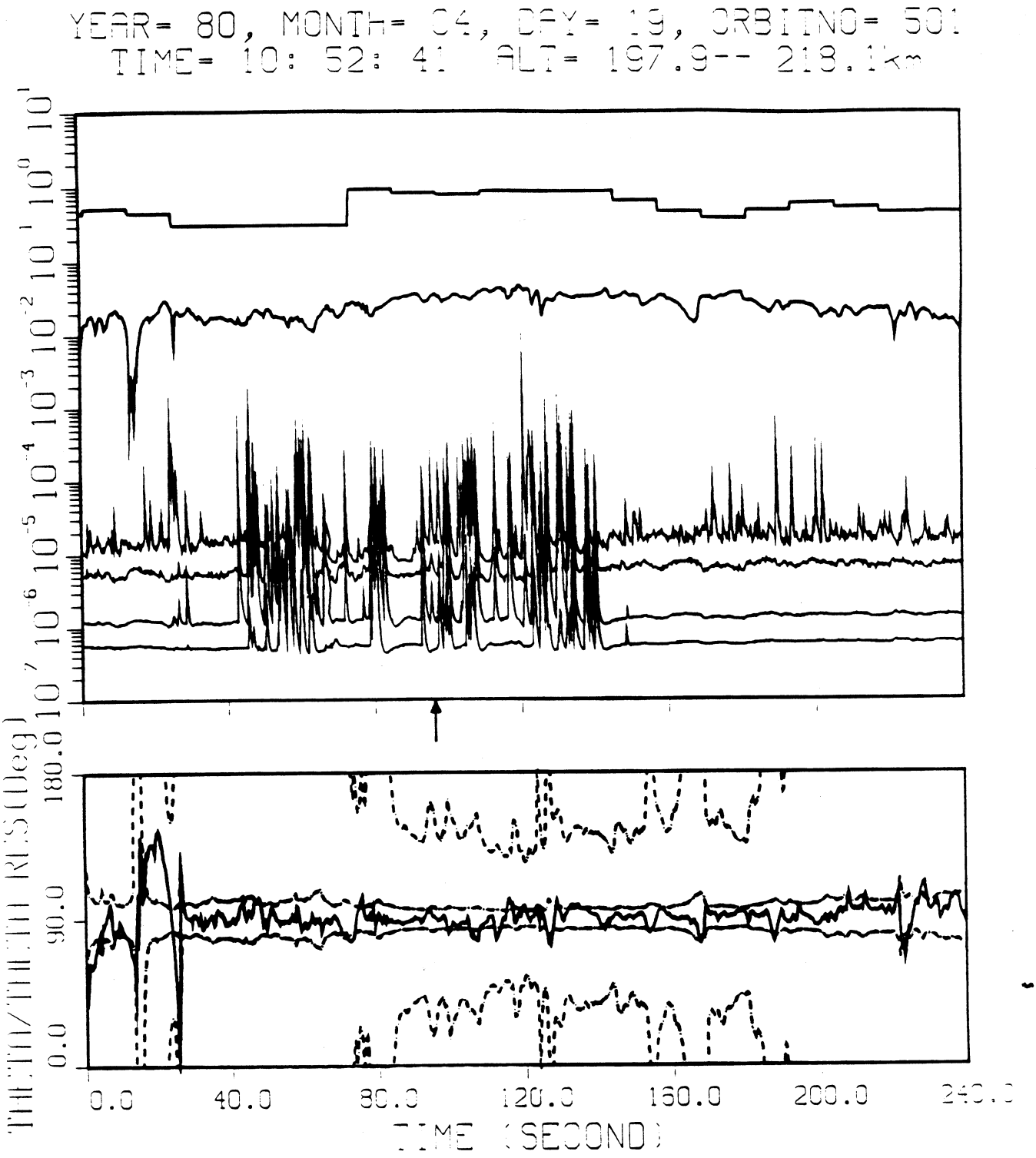

Fig 5f

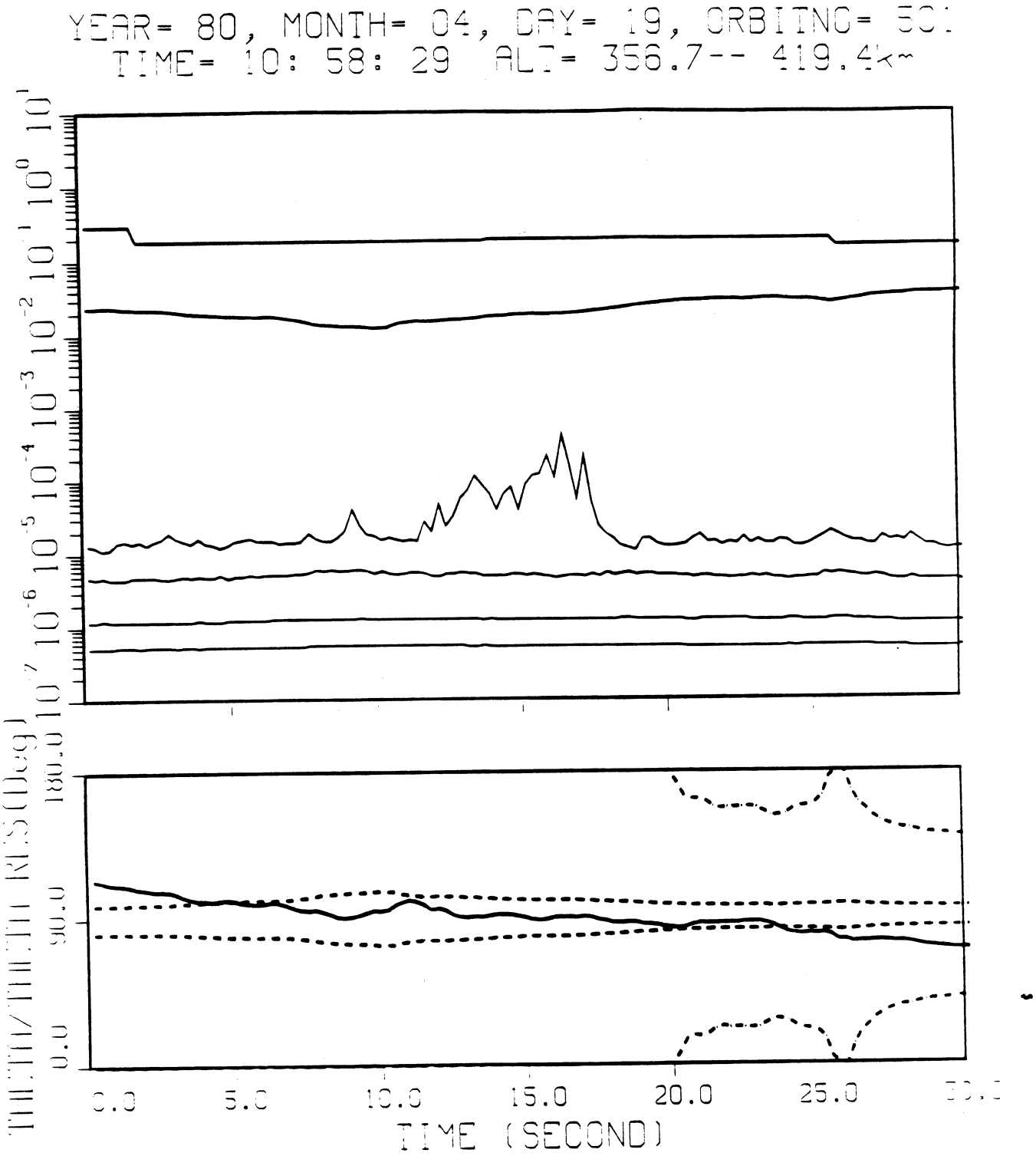

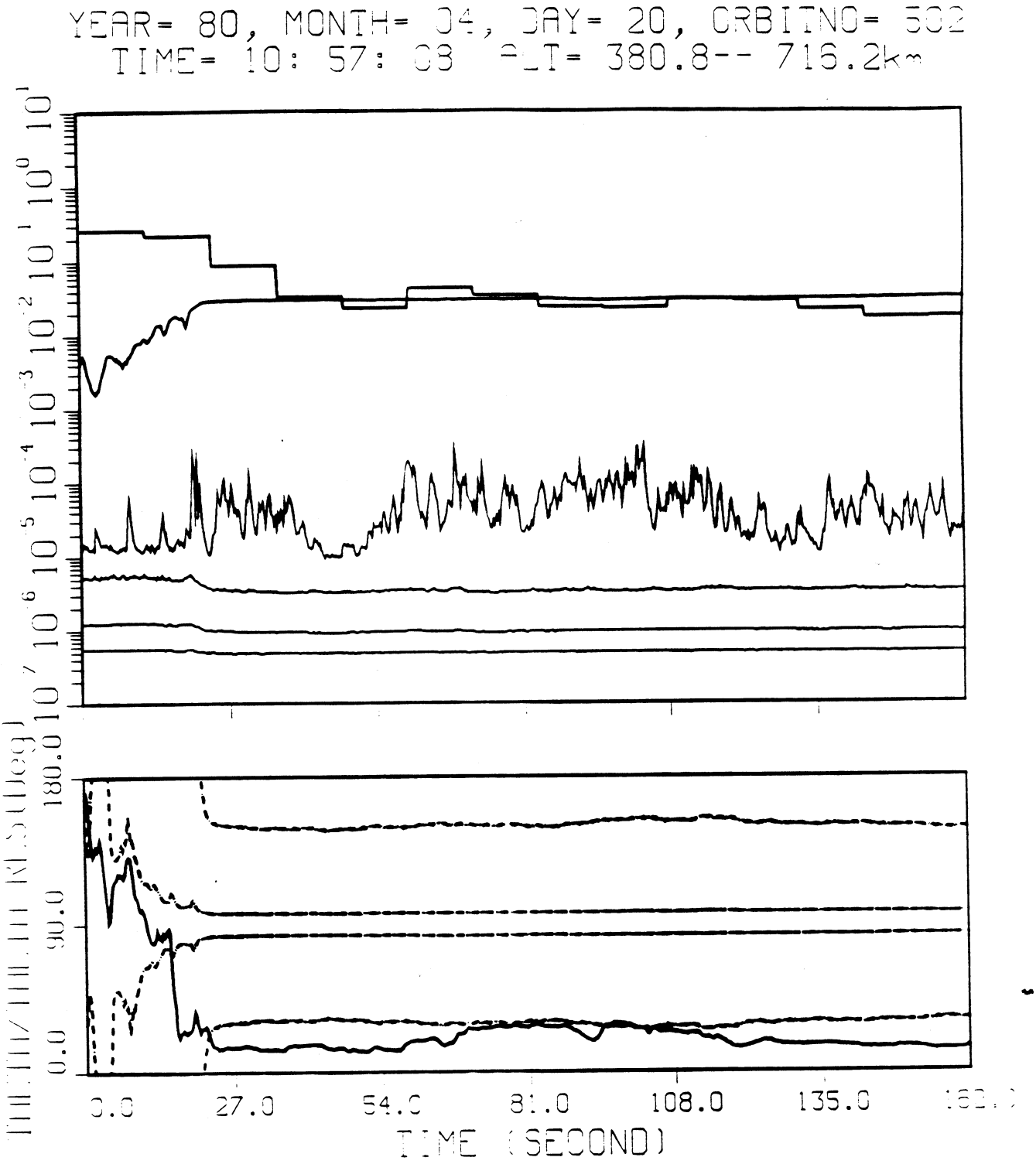

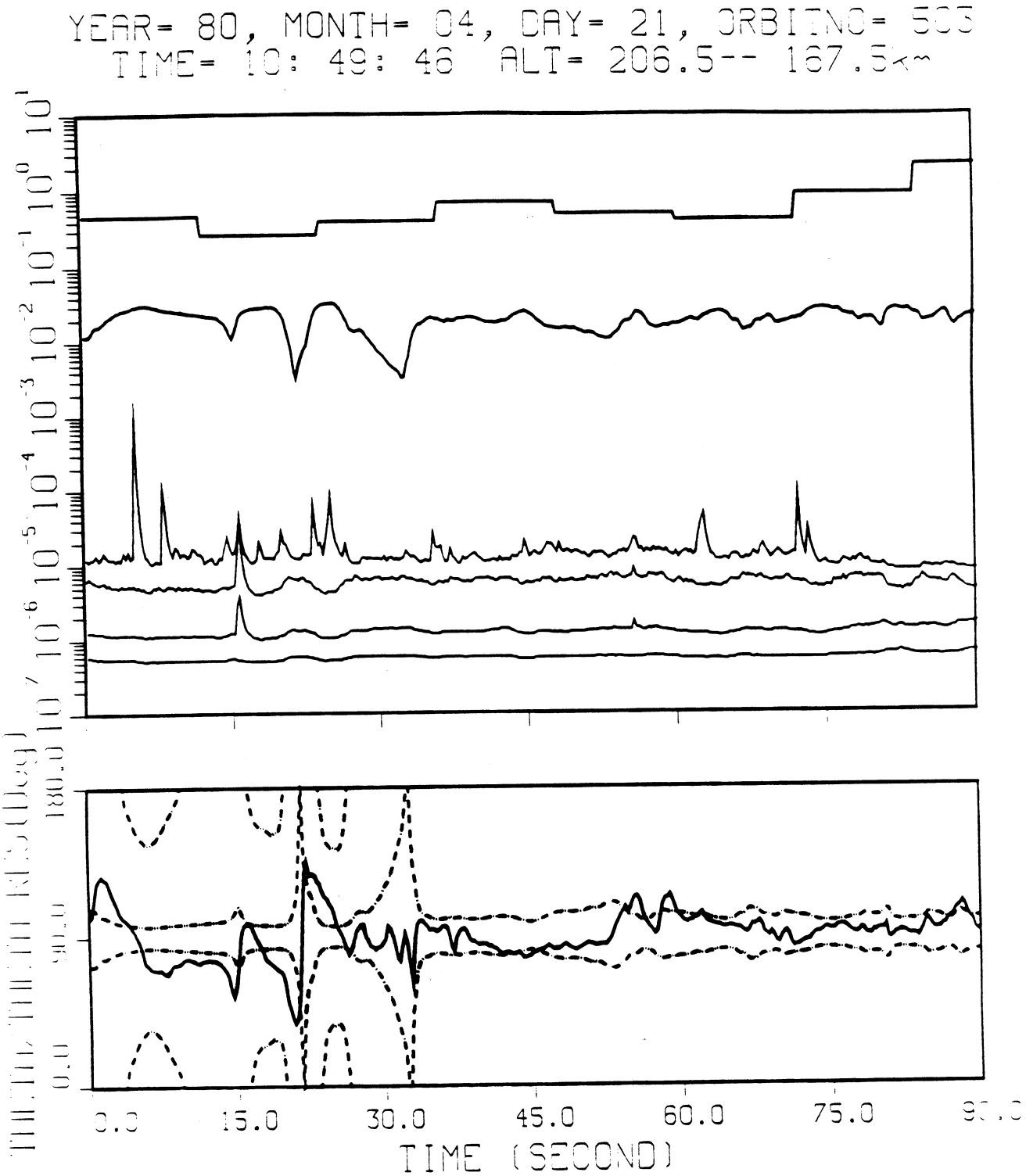

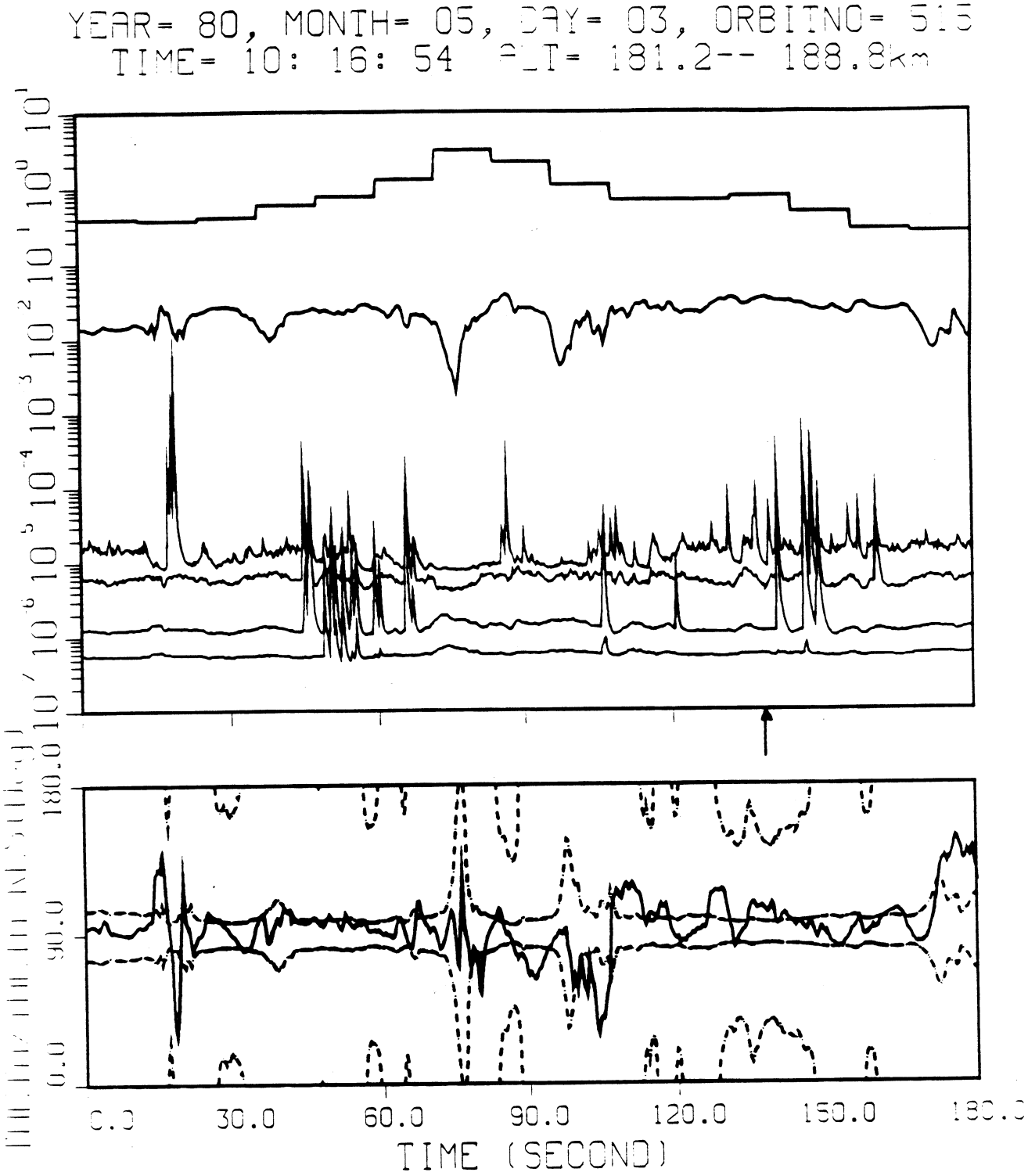

Fig 5)

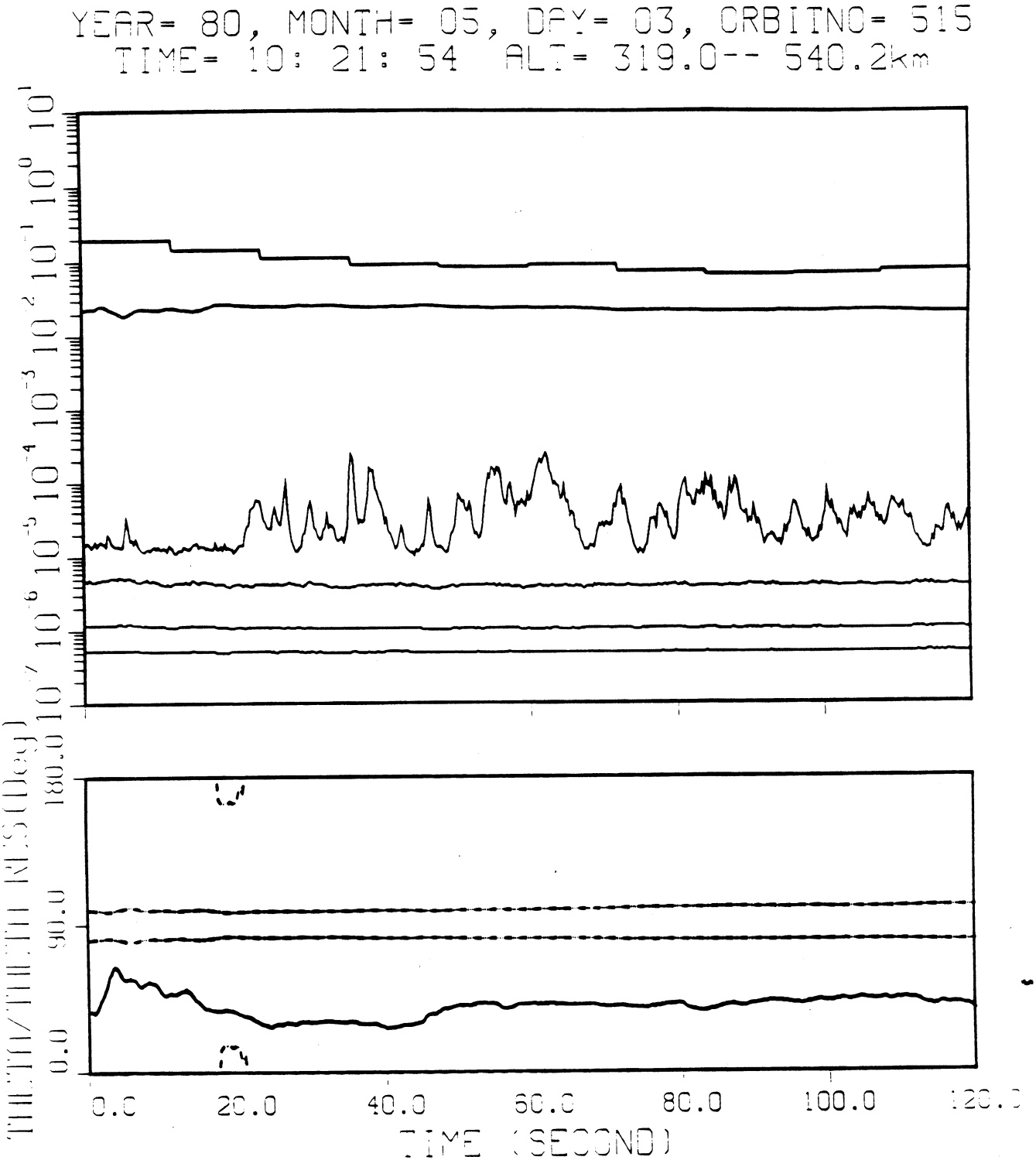

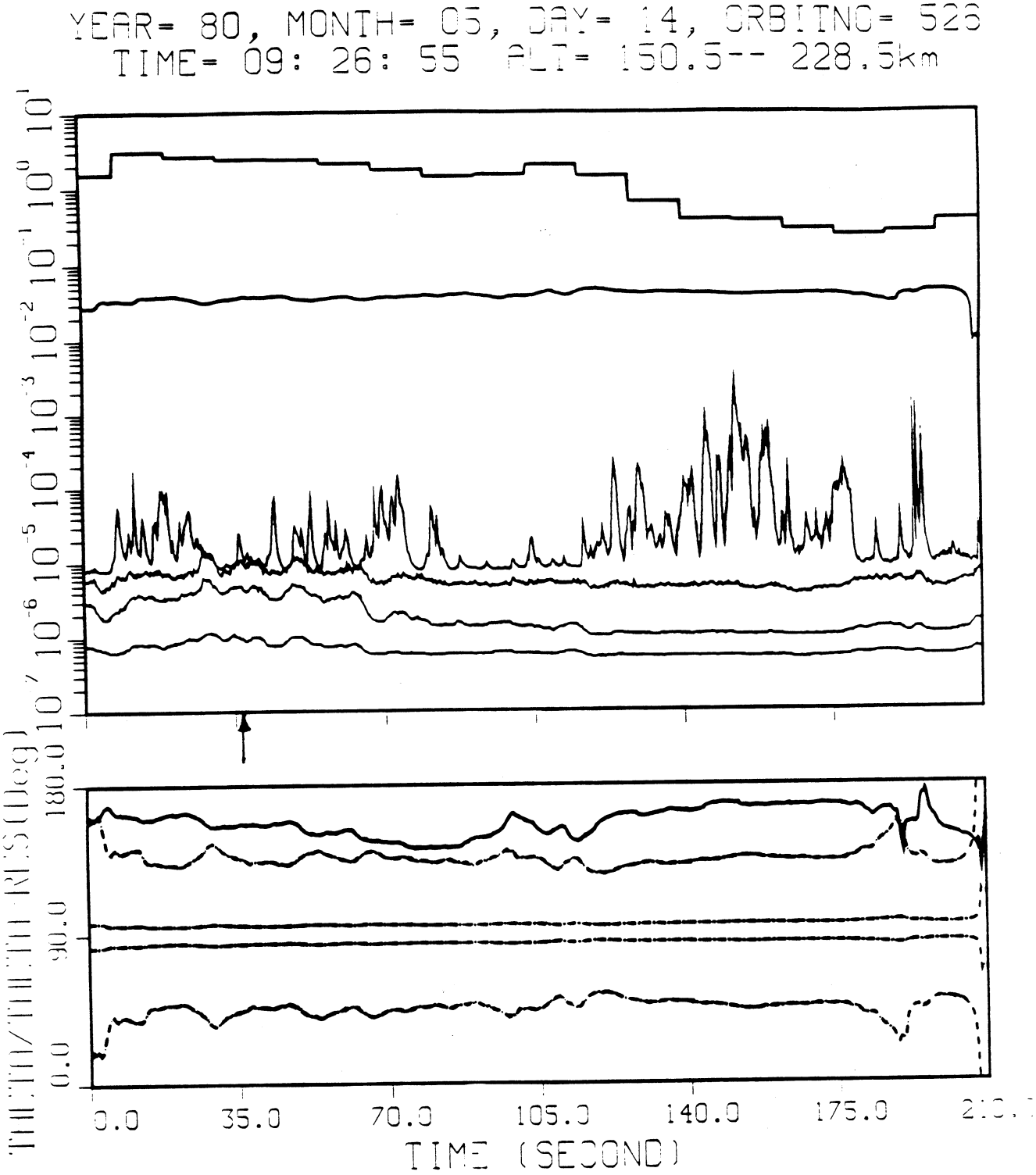

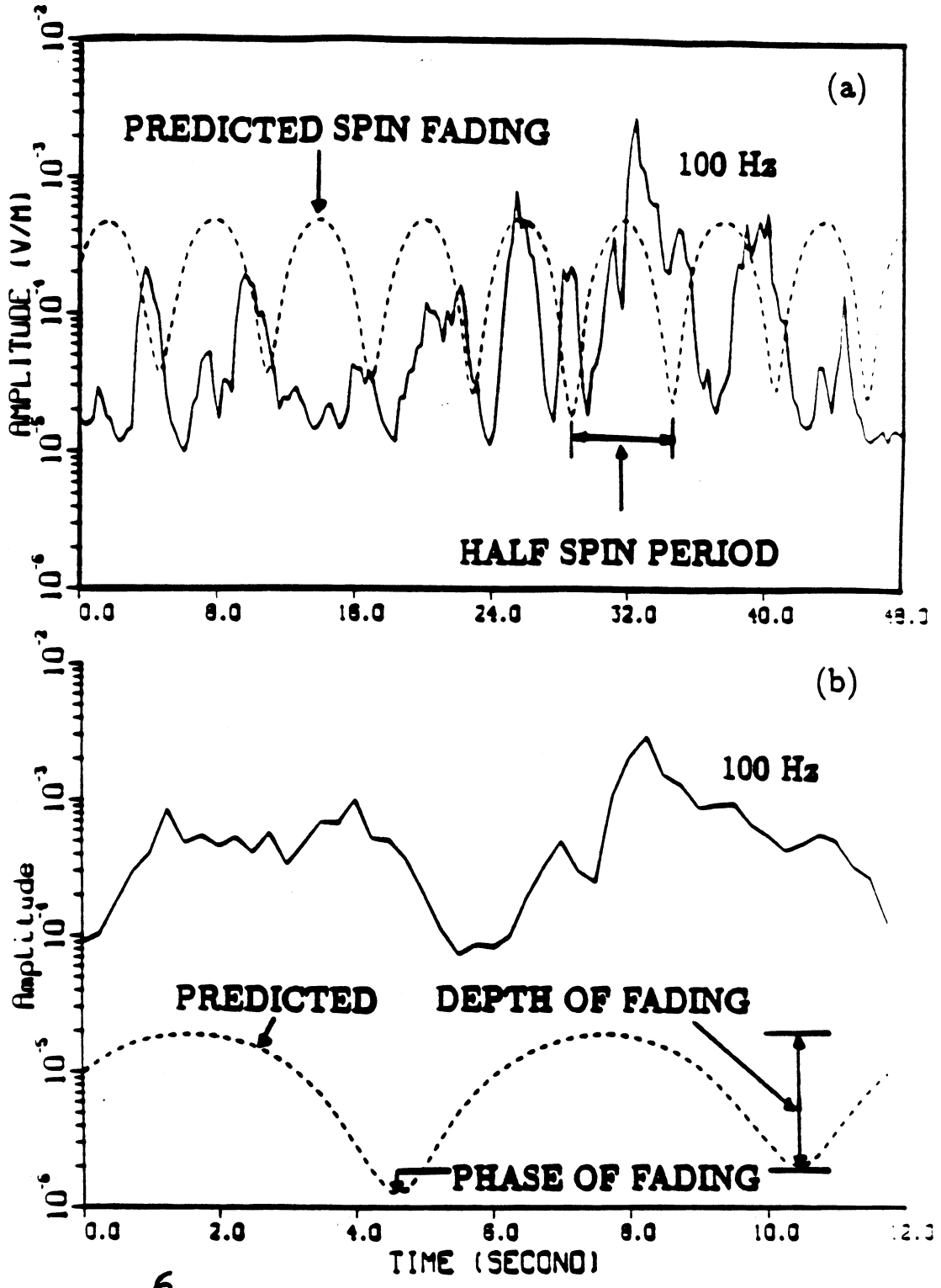

Figure 6. (a) The predicted spin fading for the 100 Hz signal at 09:28:55 UT when the wave normal direction (Figure 2 b) was fairly steady. (b) The predicted spin fading and data averaged over four spin cycles. The spin period is 12 s. Well defined spin fading at twice the spin frequency, as predicted theoretically is seen in the averaged data.

Fig 7a

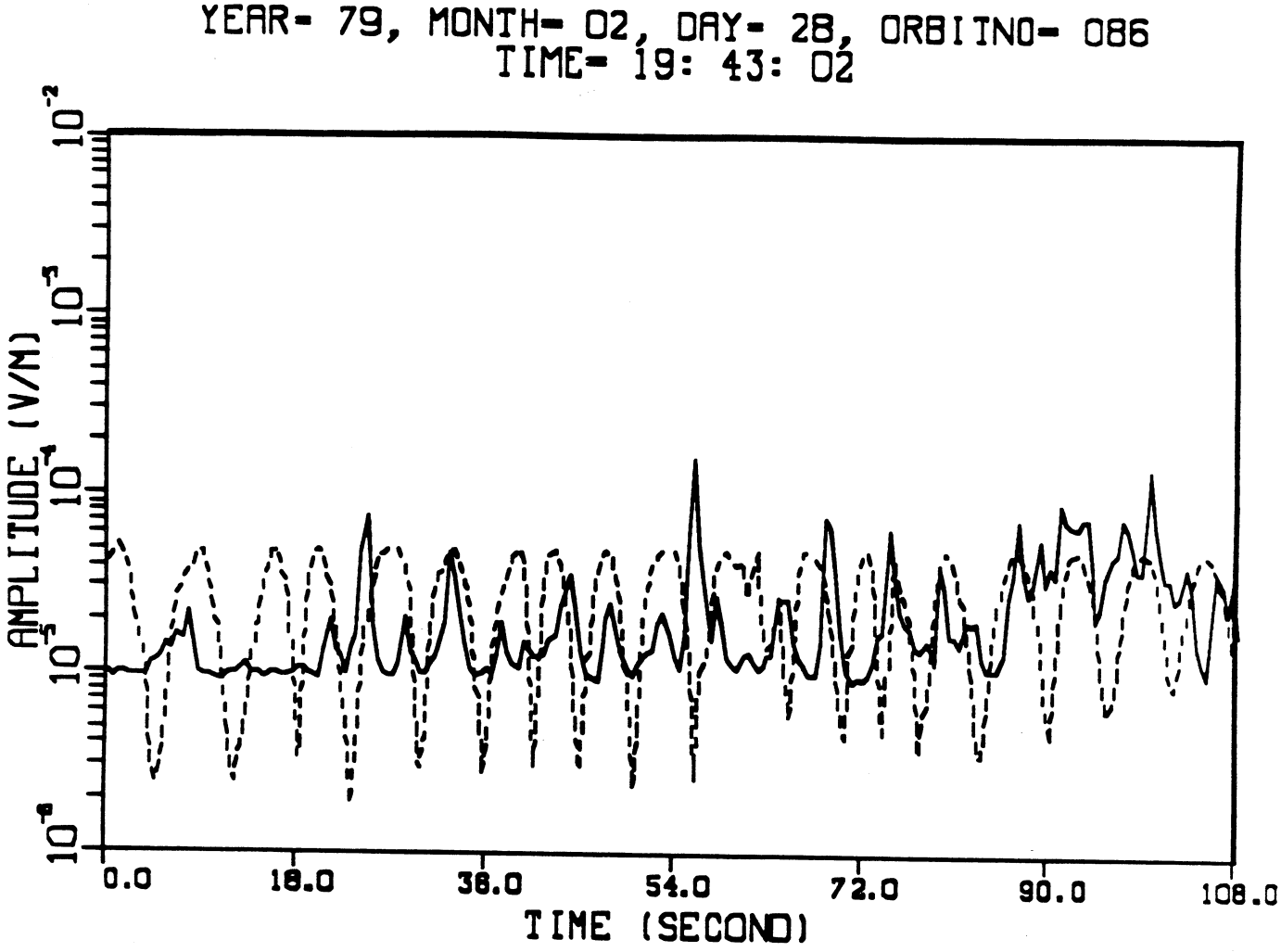
YEAR= 79, MONTH= 02, DAY= 28, ORBITNO= 086
TIME= 19: 43: 02
AMPLITUDE (V/M)
10^{-2}
10^{-3}
10^{-4}
10^{-5}
10^{-6}
0.0
18.0
36.0
54.0
72.0
90.0
108.0
TIME (SECOND)

Fig 7b

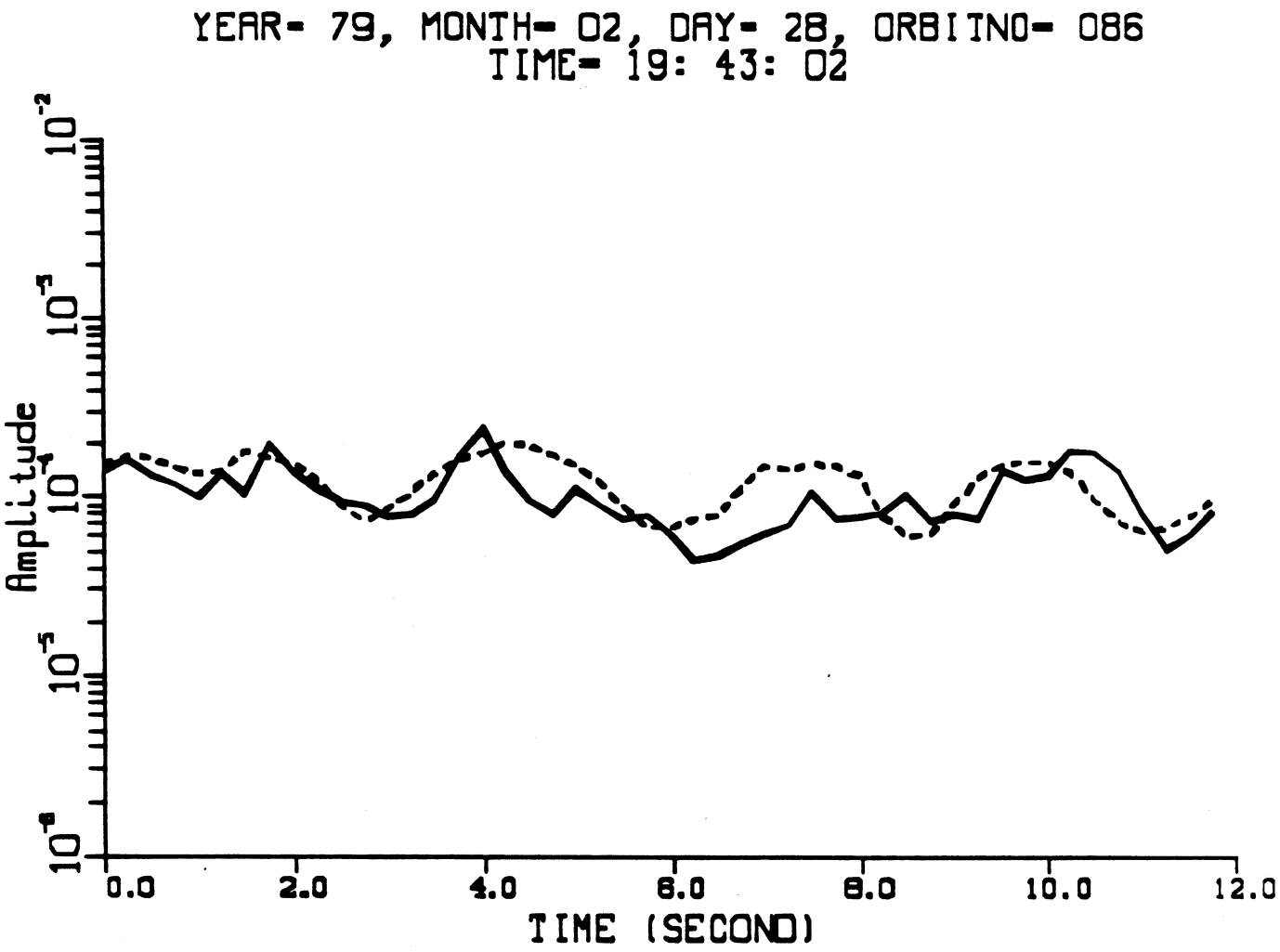
YEAR= 79, MONTH= 02, DAY= 28, ORBITNO= 086
TIME= 19: 43: 02
Amplitude
10^{-2}
10^{-3}
10^{-4}
10^{-5}
10^{-6}
0.0
2.0
4.0
6.0
8.0
10.0
12.0
TIME (SECOND)

19 APR 1980 PVO (OEFD) 10:54:05 UT
PERIAPSIS: 10:54:17 UT, ALT=155.6 KM, SZA=143.58

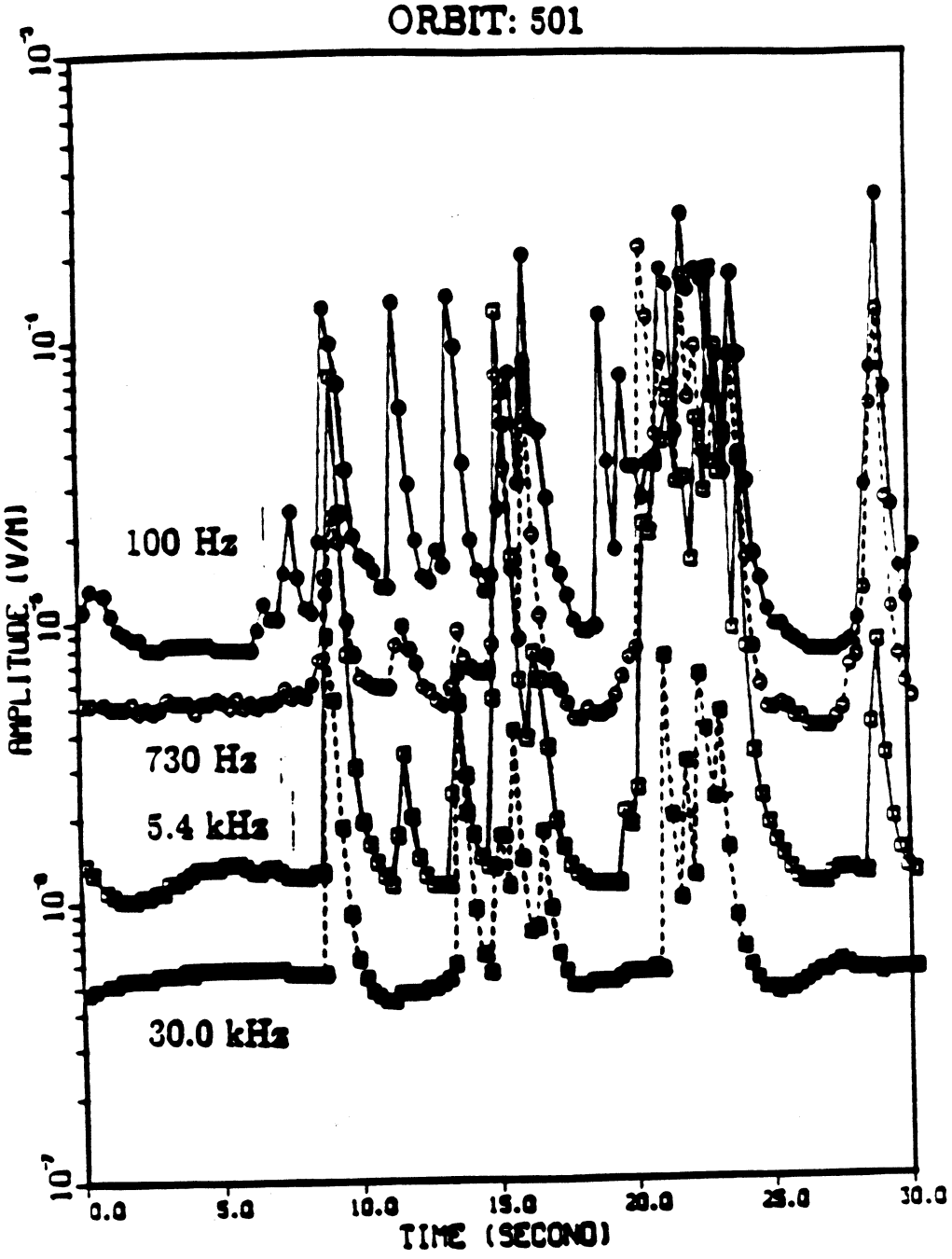

Figure 8. Display on an expanded time scale of a close correlation among the plasma wave data in four frequency channels for orbit 501.